DYNAMO Sub Surface data from the R/V Revelle

Moum, James N.*   jnmoum@coas.oregonstate.edu

Professor, Oregon State University, College of Earth, Ocean, and Atmospheric Sciences
104 CEOAS Admin Bldg, Corvallis OR 97331-5503

Kerns, Brandon W.^   bkerns@uw.edu

Senior Meteorologist, University of Washington Applied Physics Laboratory
1013 NE 40 ST, BOX 355640, Seattle, Washington, 98105-6698.

*Principal Investigator
^Prepared this document

1. Data Set Overview:

The R/V *Revelle* was dispatched during CINDY/DYNAMO to make air-sea observations in the central equatorial Indian Ocean. The ship also deployed three pairs of surface and subsurface moorings and a sea glider (data documentation separate). As part of DYNAMO, Revelle's primary functions have been as the NE component in the main array of 4 sounding stations and as a base for C--band radar observations of precipitating cloud activity. Revelle was the principal observational base for investigation of direct air-sea interactions associated with initiation and propagation of the Madden-Julian Oscillation (MJO) in the central equatorial Indian Ocean. Subsurface ocean observations were focused on ocean mixing and optics. This collection is for the ocean mixing data. It includes a full MJO cycle including a cyclone assisted MJO westerly wind burst.

<u>Time period</u>: 4 October – 7 December 2011 (Cruise legs 2 and 3).

<u>Physical location</u>: The on-station location for the R/V *Revelle* was 80.5°E, 0°N. The R/V *Revelle* DYNAMO cruise was broken in to four legs. The data in this collection were collected during legs 2 and 3, with ship tracks indicated below:
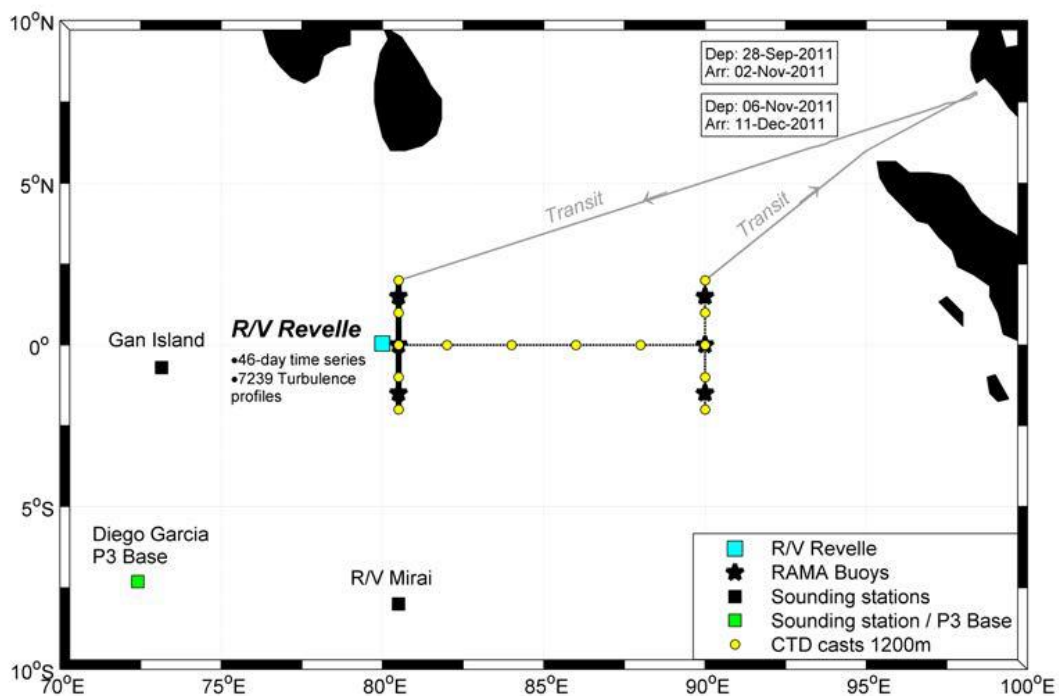
2. Instrument Description

Various observation platforms were deployed from the R/V *Revelle*, as follows:

Instrument	Measurements
ADCP (RD Instruments Narrowband 150 kHz)	currents
Ship's CTD	temperature, salinity, conductivity, pressure, oxygen, fluorescence. Twice daily to 1000 m.
OSU Chameleon	temperature, salinity, conductivity, oxygen, nitrogen, fluorescence, microscale turbulence.

3. Data Collection and Processing

Data were provided by the PI in Matlab ".mat" format. Brandon Kerns converted the data in to NetCDF. CTD data were provided as separate files for each cast, and this convention was retained. ADCP and Chameleon data were provided as one file per cruise leg, and this convention was retained. Additional quality control was not performed.

4. Data Format

4.1. ADCP

ADCP data are in NetCDF format with one file for each cruise leg (legs 2 and 3).

```
dimensions:
        time = 540 ;
        depth = 35 ;
variables:
        double depth(depth) ;
                depth:units = "m" ;
                depth:standard_name = "depth" ;
                depth:long_name = "Depth" ;
                depth:original_name = "z" ;
        double time(time) ;
                time:units = "seconds since 1970-1-1 0:00:00 0:00" ;
                time:notes = "Matlab datenum converted to UNIX time stamp." ;
        double decimal_day(time) ;
                decimal_day:units = "days since 2011-1-1 0:00:00 0:00" ;
                decimal_day:notes = "Matlab datenum converted to decimal days (0.00 --
> 0000 UTC 1 Jan. 2011)." ;
        double u(depth, time) ;
                u:units = "m s-1" ;
                u:standard_name = "eastward_sea_water_velocity" ;
                u:long_name = "Eastward Sea Water Velocity Component" ;
                u:original_name = "u" ;
        double v(depth, time) ;
                v:units = "m s-1" ;
                v:standard_name = "northward_sea_water_velocity" ;
                v:long_name = "Northward Sea Water Velocity Component" ;
                v:original_name = "v" ;

// global attributes:
```

```
                :Conventions = "CF-1.7" ;
                :title = "DYNAMO Revelle ADCO Data: Dynamo Legacy Collection" ;
                :institution = "JAMSTEC" ;
                :contact = "Jim Moum (moum@coas.oregonstate.edu), Brandon Kerns
(bkerns@uw.edu)" ;
                :data_PI = "Jim Moum (moum@coas.oregonstate.edu)" ;
                :source = "ADCP profiles" ;
                :history = "Brandon Kerns obtained the data from Jim Moum in February
2018 and converted from Matlab format to netcdf format." ;
                :references = "" ;
                :comment = "ADCP was deployed by the R/V Revelle during legs 2 and 3
of the CINDY/DYNAMO field campaign, from October to December 2011. This file contains
all the ADCP profiles for one cruise leg. Original file name:
adcp150_nofish_1hr_leg2.mat." ;
}
```

4.2. CTD

CTD data are in NetCDF format with one file for each cast.

```
dimensions:
        count = 24747 ;
        cast = 1 ;
variables:
        int64 castno(cast) ;
                castno:units = "1" ;
                castno:long_name = "Cast Number" ;
        double latitude(cast) ;
                latitude:units = "degrees_lat" ;
                latitude:long_name = "Cast Latitude" ;
        double longitude(cast) ;
                longitude:units = "degrees_longitude" ;
                longitude:long_name = "Cast Longitude" ;
        int64 count(count) ;
                count:units = "1" ;
                count:notes = "Observation Count." ;
        double time(count) ;
                time:units = "hours since 1970-1-1 0:00:00 0:00" ;
                time:notes = "Matlab datenum converted to UNIX time stamp." ;
        double decimal_day(count) ;
                decimal_day:units = "days since 2011-1-1 0:00:00 0:00" ;
                decimal_day:notes = "Matlab datenum converted to decimal days (0.00 --
> 0000 UTC 1 Jan. 2011)." ;
        double pressure(count) ;
                pressure:units = "db" ;
                pressure:standard_name = "sea_water_pressure" ;
                pressure:long_name = "Sea Water Pressure" ;
                pressure:original_name = "pressure" ;
        double depth(count) ;
                depth:units = "m" ;
                depth:standard_name = "depth" ;
                depth:long_name = "Depth" ;
                depth:original_name = "depth" ;
        double t(count) ;
                t:units = "Celsius" ;
                t:standard_name = "sea_water_temperature" ;
                t:long_name = "Sea Water Temperature" ;
                t:original_name = "temp1" ;
        double t2(count) ;
                t2:units = "Celsius" ;
                t2:standard_name = "sea_water_temperature" ;
                t2:long_name = "Sea Water Temperature 2" ;
```

```
                t2:original_name = "temp2" ;
        double s(count) ;
                s:units = "PSU" ;
                s:standard_name = "sea_water_salinity" ;
                s:long_name = "Sea Water Salinity" ;
                s:original_name = "sal1" ;
        double s2(count) ;
                s2:units = "PSU" ;
                s2:standard_name = "sea_water_salinity" ;
                s2:long_name = "Sea Water Salinity 2" ;
                s2:original_name = "sal2" ;
        double cond(count) ;
                cond:units = "S m-1" ;
                cond:standard_name = "sea_water_electrical_conductivity" ;
                cond:long_name = "Sea Water Electrical Conductivity" ;
                cond:original_name = "cond1" ;
        double cond2(count) ;
                cond2:units = "S m-1" ;
                cond2:standard_name = "sea_water_electrical_conductivity" ;
                cond2:long_name = "Sea Water Electrical Conductivity 2" ;
                cond2:original_name = "cond2" ;
        double oxygen(count) ;
                oxygen:units = "mol L-1" ;
                oxygen:standard_name = "mass_concentration_of_oxygen_in_sea_water" ;
                oxygen:long_name = "Oxygen Content" ;
                oxygen:original_name = "oxygen_ml_l" ;
        double oxygen_perc_sat(count) ;
                oxygen_perc_sat:units = "percent" ;
                oxygen_perc_sat:standard_name =
"fractional_saturation_of_oxygen_in_sea_water" ;
                oxygen_perc_sat:long_name = "Oxygen Saturation Percent" ;
                oxygen_perc_sat:original_name = "oxygen_perc_saturation" ;
        double fluorsecence(count) ;
                fluorsecence:units = "ug l-1" ;
                fluorsecence:standard_name = "" ;
                fluorsecence:long_name = "Flourescence, Seapoint" ;
                fluorsecence:original_name = "fluorescence_seapoint" ;
        double beam_attenuation_1_over_m(count) ;
                beam_attenuation_1_over_m:units = "m-1" ;
                beam_attenuation_1_over_m:standard_name = "" ;
                beam_attenuation_1_over_m:long_name = "Beam Attenuation" ;
                beam_attenuation_1_over_m:original_name = "beam_attenuation_1_over_m"
;
        double beam_transmission_perc(count) ;
                beam_transmission_perc:units = "percent" ;
                beam_transmission_perc:standard_name = "" ;
                beam_transmission_perc:long_name = "Beam Transmission" ;
                beam_transmission_perc:original_name = "beam_transmission_perc" ;

// global attributes:
                :Conventions = "CF-1.7" ;
                :title = "R/V Revelle CTD Data: Dynamo Legacy Collection" ;
                :institution = "JAMSTEC" ;
                :contact = "Jim Moum (moum@coas.oregonstate.edu), Brandon Kerns
(bkerns@uw.edu)" ;
                :data_PI = "Jim Moum (moum@coas.oregonstate.edu)" ;
                :source = "CTD profiles" ;
                :history = "Brandon Kerns obtained the data from Jim Moum in February
2018 and converted from Matlab format to netcdf format. CAUTION: There are some
strange temperature and salinity values that have not been QCd out." ;
                :references = "" ;
                :comment = "CTDs were deployed by the R/V Revelle during the
CINDY/DYNAMO field campaign from September to December 2011. This file contains a
```

```
single CTD cast (down then up). ReadMe.txt file states: Seabird2 in CTD 1,2 is bad.
Original file name: CTD19.mat." ;
}
```

4.3.   Chameleon

Chameleon data are in NetCDF format with one file for each cruise leg (legs 2 and 3).

```
dimensions:
        time = 3559 ;
        depth = 350 ;
variables:
        double depth(depth) ;
                depth:units = "m" ;
                depth:long_name = "Depth" ;
        double time(time) ;
                time:units = "seconds since 1970-1-1 0:00:00 0:00" ;
                time:notes = "Matlab datenum converted to UNIX time stamp. This
appears to represent the average time of the profile. Also see start_time and
end_time." ;
        double decimal_day(time) ;
                decimal_day:units = "days since 2011-1-1 0:00:00 0:00" ;
                decimal_day:notes = "Matlab datenum converted to decimal days (0.00 --
> 0000 UTC 1 Jan. 2011).  This appears to represent the average time of the profile.
Also see start_decimal_day and end_decimal_day." ;
        double start_time(time) ;
                start_time:units = "seconds since 1970-1-1 0:00:00 0:00" ;
                start_time:long_name = "Profile Start Time" ;
                start_time:notes = "String converted to UNIX time stamp." ;
        double start_decimal_day(time) ;
                start_decimal_day:units = "days since 2011-1-1 0:00:00 0:00" ;
                start_decimal_day:notes = "String converted to decimal days (0.00 -->
0000 UTC 1 Jan. 2011)." ;
        double end_time(time) ;
                end_time:units = "seconds since 1970-1-1 0:00:00 0:00" ;
                end_time:long_name = "Profile End Time" ;
                end_time:notes = "String converted to UNIX time stamp." ;
        double end_decimal_day(time) ;
                end_decimal_day:units = "days since 2011-1-1 0:00:00 0:00" ;
                end_decimal_day:notes = "String converted to decimal days (0.00 -->
0000 UTC 1 Jan. 2011)." ;
        int64 castno(time) ;
                castno:units = "1" ;
                castno:long_name = "Cast Number" ;
        double latitude(time) ;
                latitude:units = "degrees_north" ;
                latitude:standard_name = "latitude" ;
                latitude:long_name = "latitude" ;
                latitude:original_name = "lat" ;
        double longitude(time) ;
                longitude:units = "degrees_east" ;
                longitude:standard_name = "longitude" ;
                longitude:long_name = "longitude" ;
                longitude:original_name = "lon" ;
        double pmax(time) ;
                pmax:units = "db" ;
                pmax:standard_name = "" ;
                pmax:long_name = "Maximum Pressure" ;
                pmax:original_name = "pmax" ;
        double mld(time) ;
                mld:units = "m" ;
                mld:standard_name = "ocean_mixed_layer_thickness" ;
```

```
        mld:long_name = "Mixed Layer Depth" ;
        mld:original_name = "mld" ;
double t(depth, time) ;
        t:units = "Celsius" ;
        t:standard_name = "sea_water_temperature" ;
        t:long_name = "Sea Water Temperature" ;
        t:original_name = "T" ;
double t2(depth, time) ;
        t2:units = "Celsius" ;
        t2:standard_name = "sea_water_temperature" ;
        t2:long_name = "Sea Water Temperature 2" ;
        t2:original_name = "T2" ;
double theta(depth, time) ;
        theta:units = "Celsius" ;
        theta:standard_name = "sea_water_potential_temperature" ;
        theta:long_name = "Sea Water Potential Temperature" ;
        theta:original_name = "THETA" ;
double s(depth, time) ;
        s:units = "PSU" ;
        s:standard_name = "sea_water_salinity" ;
        s:long_name = "Sea Water Salinity" ;
        s:original_name = "S" ;
double pressure(depth, time) ;
        pressure:units = "db" ;
        pressure:standard_name = "sea_water_pressure" ;
        pressure:long_name = "Sea Water Pressure" ;
        pressure:original_name = "P" ;
double conductivity(depth, time) ;
        conductivity:units = "S m-1" ;
        conductivity:standard_name = "sea_water_electrical_conductivity" ;
        conductivity:long_name = "Sea Water Conductivity" ;
        conductivity:original_name = "C" ;
double ax_tilt(depth, time) ;
        ax_tilt:units = "" ;
        ax_tilt:standard_name = "" ;
        ax_tilt:long_name = "" ;
        ax_tilt:original_name = "AX_TILT" ;
double ay_tilt(depth, time) ;
        ay_tilt:units = "" ;
        ay_tilt:standard_name = "" ;
        ay_tilt:long_name = "" ;
        ay_tilt:original_name = "AY_TILT" ;
double az2(depth, time) ;
        az2:units = "" ;
        az2:standard_name = "" ;
        az2:long_name = "" ;
        az2:original_name = "AZ2" ;
double chi(depth, time) ;
        chi:units = "" ;
        chi:standard_name = "" ;
        chi:long_name = "" ;
        chi:original_name = "CHI" ;
double dsdz(depth, time) ;
        dsdz:units = "" ;
        dsdz:standard_name = "" ;
        dsdz:long_name = "" ;
        dsdz:original_name = "DSDZ" ;
double dsdz_rhoorder(depth, time) ;
        dsdz_rhoorder:units = "" ;
        dsdz_rhoorder:standard_name = "" ;
        dsdz_rhoorder:long_name = "" ;
        dsdz_rhoorder:original_name = "DSDZ_RHOORDER" ;
double dtdz(depth, time) ;
```

```
        dtdz:units = "" ;
        dtdz:standard_name = "" ;
        dtdz:long_name = "" ;
        dtdz:original_name = "DTDZ" ;
double dtdz_rhoorder(depth, time) ;
        dtdz_rhoorder:units = "" ;
        dtdz_rhoorder:standard_name = "" ;
        dtdz_rhoorder:long_name = "" ;
        dtdz_rhoorder:original_name = "DTDZ_RHOORDER" ;
double epsilon(depth, time) ;
        epsilon:units = "" ;
        epsilon:standard_name = "" ;
        epsilon:long_name = "" ;
        epsilon:original_name = "EPSILON" ;
double epsilon1(depth, time) ;
        epsilon1:units = "" ;
        epsilon1:standard_name = "" ;
        epsilon1:long_name = "" ;
        epsilon1:original_name = "EPSILON1" ;
double epsilon2(depth, time) ;
        epsilon2:units = "" ;
        epsilon2:standard_name = "" ;
        epsilon2:long_name = "" ;
        epsilon2:original_name = "EPSILON2" ;
double fallspd(depth, time) ;
        fallspd:units = "" ;
        fallspd:standard_name = "" ;
        fallspd:long_name = "" ;
        fallspd:original_name = "FALLSPD" ;
double mhc(depth, time) ;
        mhc:units = "" ;
        mhc:standard_name = "" ;
        mhc:long_name = "" ;
        mhc:original_name = "MHC" ;
double n2(depth, time) ;
        n2:units = "" ;
        n2:standard_name = "" ;
        n2:long_name = "" ;
        n2:original_name = "N2" ;
double scat(depth, time) ;
        scat:units = "" ;
        scat:standard_name = "" ;
        scat:long_name = "" ;
        scat:original_name = "SCAT" ;
double sigma(depth, time) ;
        sigma:units = "" ;
        sigma:standard_name = "" ;
        sigma:long_name = "" ;
        sigma:original_name = "SIGMA" ;
double tp(depth, time) ;
        tp:units = "" ;
        tp:standard_name = "" ;
        tp:long_name = "" ;
        tp:original_name = "TP" ;
double varaz(depth, time) ;
        varaz:units = "" ;
        varaz:standard_name = "" ;
        varaz:long_name = "" ;
        varaz:original_name = "VARAZ" ;
double varlt(depth, time) ;
        varlt:units = "" ;
        varlt:standard_name = "" ;
        varlt:long_name = "" ;
```

```
                varlt:original_name = "VARLT" ;

// global attributes:
                :Conventions = "CF-1.7" ;
                :title = "R/V Revelle Chameleon Data: Dynamo Legacy Collection" ;
                :institution = "OSU" ;
                :contact = "Jim Moum (moum@coas.oregonstate.edu), Brandon Kerns
(bkerns@uw.edu)" ;
                :data_PI = "Jim Moum (moum@coas.oregonstate.edu)" ;
                :source = "Chameleon deployed by R/V Revelle" ;
                :history = "Brandon Kerns obtained the data from Jim Moum in February
2018 and converted from Matlab format to netcdf format. The \"bottom\" variable was
not included since it was all nan." ;
                :references = "" ;
                :comment = "Chameleon was deployed by the R/V Revelle during the
CINDY/DYNAMO field campaign from September to December 2011. This file contains the
Chameleon data for one cruise leg. Original file name: cham_leg2.mat." ;
}
```

5. Data Remarks

The data can be accessed using the myriad of software that is able to interact with NetCDF format files, including ncdump, ncview, Matlab, Python, IDL, and NCL.

Quality control has not been carried out beyond what was provided by the PI.

6. References

de Szoeke, S.P., J.B. Edson, J.R. Marion, C.W. Fairall, and L. Bariteau, 2015: The MJO and Air–Sea Interaction in TOGA COARE and DYNAMO. J. Climate, 28, 597–622, https://doi.org/10.1175/JCLI-D-14-00477.1

Attachment: DYNAMO Leg 3 Cruise Report

December 7, 2011

This is a brief and preliminary report of work done on R/V Roger Revelle during DYNAMO Leg 3. As part of DYNAMO, Revelle's primary functions have been as the NE component in the main array of 4 sounding stations and as a base for C-band radar observations of precipitating cloud activity. Revelle was the principal observational base for investigation of direct air-sea interactions associated with initiation and propagation of the Madden-Julian Oscillation (MJO) in the central equatorial Indian Ocean.

Seven individual group reports are followed by the ship's event log that is intended as a reference to identify significant occurrences at sea. The seven groups are:

- Surface Fluxes
- Atmospheric Soundings
- Aerosols
- NOAA High-Resolution Doppler Lidar
- TOGA Radar
- Ocean Optics
- Ocean Mixing

December 7, 2011
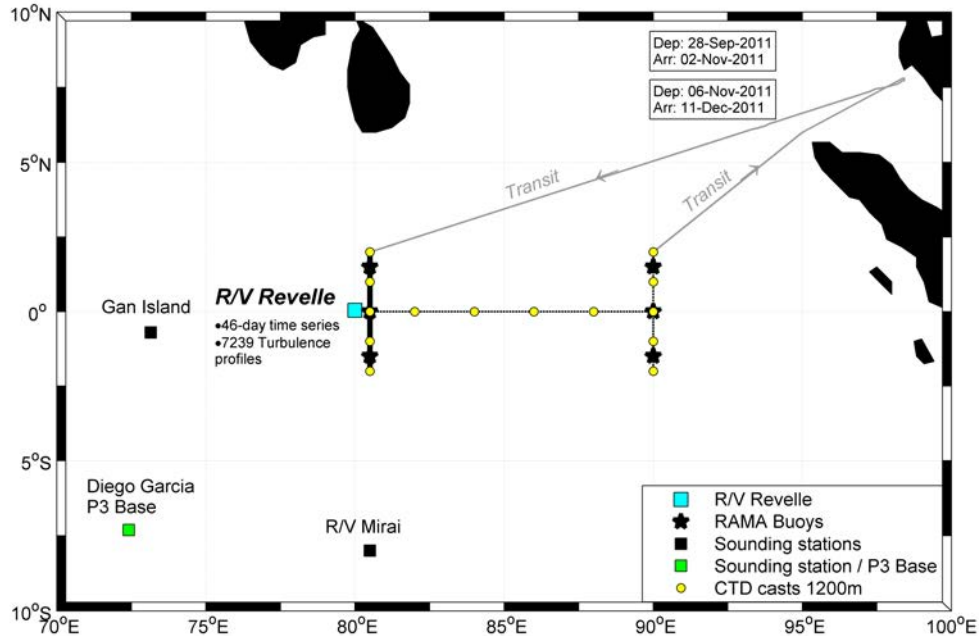
Figure 1 – Cruise track DYNAMO Legs 2,3.

Revelle left Phuket, Thailand 06 Nov 2011, and proceeded directly to 2N, 80.5E (Figure 1). An ADCP/XBT survey was conducted along 80.5 E from 2N to 2S to map out cross-equatorial current structure. Revelle returned to 0, 80.5E to conduct a 22-day time series that included measurements of surface fluxes, wind profiles, C-band radar, atmospheric soundings (8/day), aerosols, sonar-based ocean profiling and profiling of ocean structure including turbulence. These measurements included:

- continuous velocity profiling from 1 km below to 10 km above the sea surface;
- 80 CTDs;
- 7239 temperature/conductivity/turbulence upper ocean profiles to 300 m depth over 2 legs (using Chameleon);
- high-resolution eddy-correlation momentum, heat and moisture flux measurements from bow mast.
- high-resolution radiative flux measurements from radiometers and SST (using the sea-snake).

On 02 December, a large-scale CTD/ADCP transect was begun to map out the larger structure of equatorial currents as well as Kelvin and Rossby wave propagation between 80E and 90E (Figure 1).

Summary timelines for DYNAMO Legs 2,3 are included as Figure 2,3.

December 7, 2011
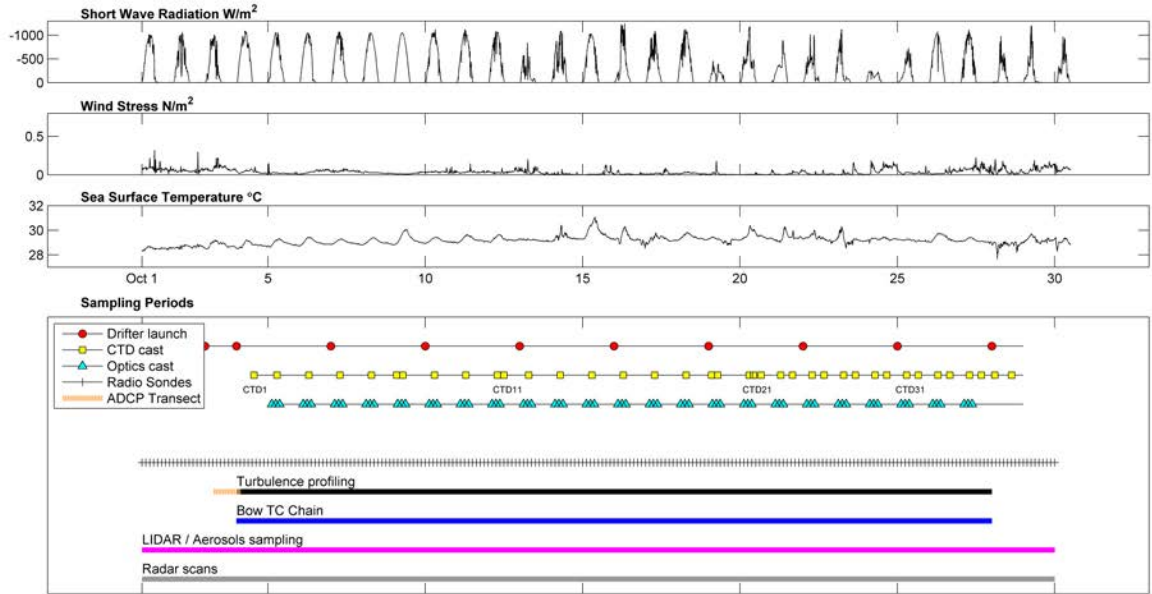
Figure 2 – Timeline DYNAMO Leg 2 / R/V Roger Revelle.
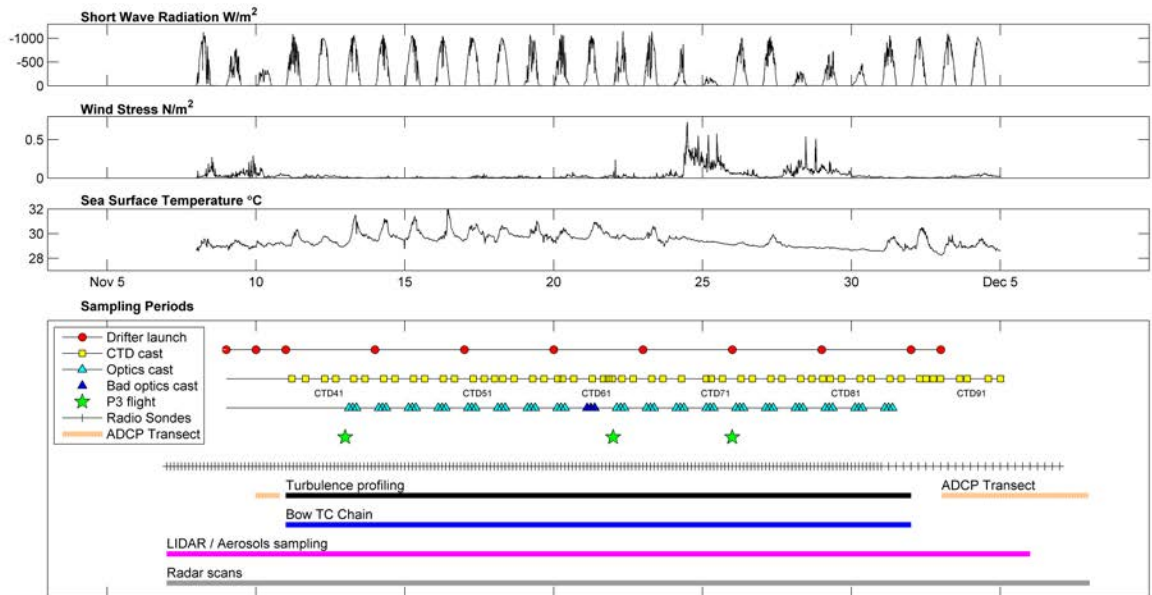
Figure 3 - Timeline DYNAMO Leg 3 / R/V Roger Revelle.

December 7, 2011

Surface Fluxes   (Jim Edson , Ludovic Bariteau, June Marion)

Leg 3 DYNAMO 2011
November 8, 2011 (Yearday 312) to December 8, 2011 (Yearday 342)
Jim Edson (UConn), Ludovic Bariteau (NOAA/PSD), and June Marion (OSU)

In situ meteorology and high-rate flux sensors operated continuously while in the sampling period for DYNAMO Leg 3. This included all sensors operating during Leg 2 with the addition of a closed-path LI-7200 IRGA to the flux systems. Sea surface temperatures were measured by the group using the sea-snake floating thermistor and radiometric estimates of skin temperature in collaboration with Chris Zappa (LDEO/Columbia).   A system to measure CO_2 concentrations in the ocean and atmosphere to support CO_2 flux measurements were made in collaboration with Wade McGillis (LDEO/Columbia). NOAA/PSD operated a suite of remote sensing instruments for low clouds and light precipitation: the NOAA W-band cloud radar, a microwave radiometer, and a laser ceilometer. Aircraft overflights were made on November 13, 22 and 26 with all systems operational and good relative winds for our flux measurement systems.

Observational Summary

The observational highlight of Leg 3 was the capture of an almost complete MJO cycle in our time series measurements. After a brief period of convective activity upon arrival, the measurements were characteristic of the suppressed phase of the MJO. Strong solar heating of the ocean overwhelmed the convective cooling by the atmosphere, and ocean surface temperature increased by approximately 1°C between 11-17 November (Yeardays 315-321).   As shown in Figure 1, winds remained light and variable during this period and little precipitation was observed. However, atmospheric convection began to increase on 17 November (Yearday 321) with precipitation falling overnight. Wind speeds and convection gradually increased during the period between 18-23 November (Yeardays 322-327). Sea surface temperatures leveled off during this period due to a gradual reduction in solar radiation and continued latent heat loss of approximately 100 Wm^{-2}. The active phase of the MJO was in full swing with the arrival of cyclone aided westerly wind burst on 24 November (Yearday 328).   Ten-minute averaged wind speeds in excess of 19 m/s where observed over growing seas with significant wave heights of approximately 3 m.   The sea-surface temperature dropped significantly during this period with combined sensible and latent heat loss to the atmosphere of approximately 200-400 Wm^{-2}. Moderate winds, precipitating convection and surface cooling continued through the end of November (Yearday 334).   Overall, precipitation exceeded evaporation during this period.   Although westerly surface winds around 5 ms^{-1} continued into December, a drying out of the atmosphere aloft and associated reduction in convective activity was observed as the active phase of the MJO-related convection moved towards the maritime continent.
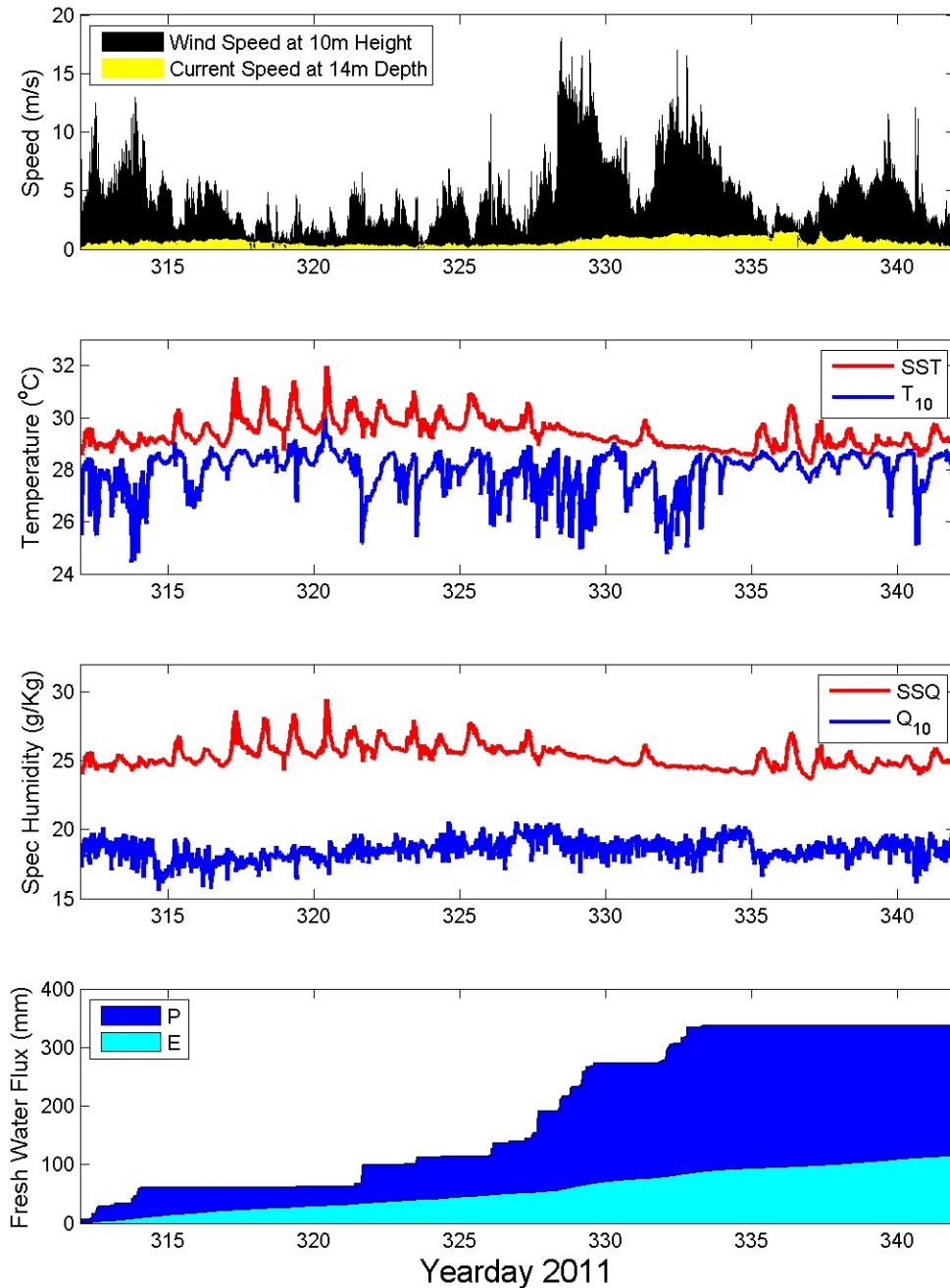
December 7, 2011

Figure 4. Time series of mean meteorological and ocean surface variable during Leg 3. The velocity data were taken from the sonic anemometers on the forward mast. Poor relative wind directions were removed and the data was interpolated through these periods. Surface currents were collected from the ship's ADCP after QC by the OSU mixing group. Air temperature was collected by two aspirated T/RH sensors on the bow. Poor relative wind directions were also removed from these data to reduce the heat island effect of the ship. Sea surface temperature was measured by the sea-snake and corrected for cool-skin effects. Precipitation (P) was provided by an optical rain gauge after calibration with 6 other rain gauges (see below). Specific humidity was calculated by combining these sensors with pressure measurements. Evaporation (E) was computed using the latent heat flux estimated by the COARE 3.0 algorithm. Accumulated totals of P and E are shown. The blue shaded area is therefore their difference.

December 7, 2011

Surface Fluxes

A summary of the latent, sensible, radiative and net heat fluxes are shown in Figure 2. The downward radiative fluxes were measured by the purgeometers (LW) and pyranometers (SW) located on the top of the forward mast.   The upward long-wave radiation was obtained using our SST measurements and corrected for IR reflection from downwelling long-wave. A commonly used parameteriztion of sea-surface albedo was used to estimate the reflected solar. The optimized set of mean meteorological and surface ocean measurements (temperature and currents) are used to compute the latent, sensible and rain fluxes with the COARE 3.0 algorithm.
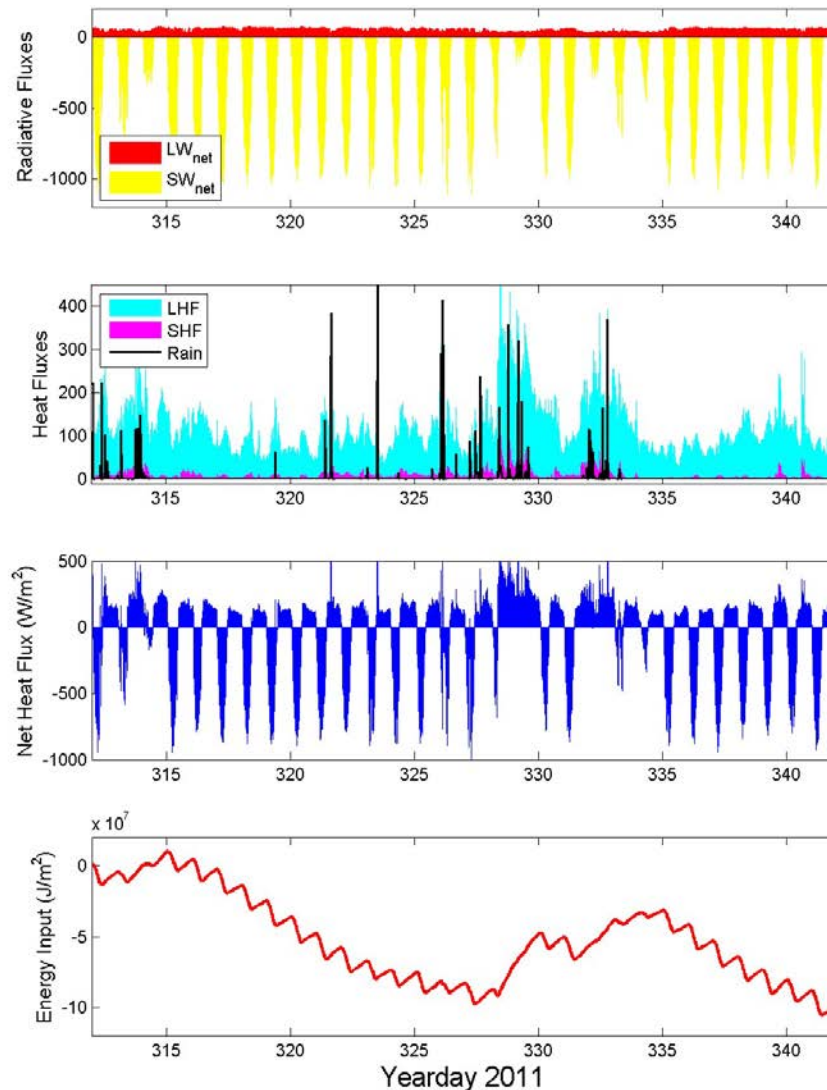
Figure 5. Time series of radiative, surface heat, and net heat fluxes during Leg 3. The lower panel shows the integral of the net heat flux over the experiment.   A small correction (~1% reduction) was applied to the short-wave measurements from the forward mast based on comparison with the PSD and OSU sensors.   A more significant correction to the long-wave measurements was applied to the mast using the PSD sensors. The latent, sensible and rain induced fluxes are computed using COARE 3.0.

December 7, 2011

The lower plot in Figure 2 shows the integrated value of the net heat flux into the ocean.   The large amount of heat supplied to the ocean during the suppressed phase of the MJO is clearly seen in the measurements between 11-20 November (Yeardays 315 and 324).   It is important to note that not all of this energy goes into heating of the mixed layer as a significant fraction of the solar radiation penetrates through this layer. Oceanic turbulence also removes some of the heat through the base of the mixed layer (see the OSU Mixing Group report for more details).   However, this still represents a significant amount of energy stored by the oceanic capacitor to potentially initiate (in tandem with favorable atmospheric condition, e.g., surface convergence and divergence aloft) and drive convection during the active phase of the MJO. This plot also shows a leveling off of the heating around 21 November (Yearday 325), which likely corresponds to the start of the active phase.   The westerly wind burst is clearly associated with the active phase, and drove the net heat loss evident between 24 November and 1 December (Yeardays 327 and 335) and associated cooling of the ocean.   The end of the time series again shows the heat supplied to the ocean (i.e., recharging of the capacitor) during the start of a new suppressed phase.   The rate of energy input is very similar to the prior period and represents the clear sky solar value integrated over a day minus the nominal value of latent heat flux of approximately 100 Wm^{-2}. The role that the ocean and air-sea exchange plays in driving the amplitude and phase of the MJO will be a focus of our collaborative investigation with the Ocean Mixing, Sounding and Remote Sensing groups.

Continued improvement to and validation of the COARE algorithm is also a goal of the experiment. Therefore, the flux group has begun to process the turbulence instrumentation on the forward mast to compute fluxes using the direct covariance (eddy correlation) method after correction for ship motion. Preliminary results from our analysis are encouraging. For example, Figure 3 shows a time series of surface stress and latent heat flux estimated from the direct covariance method and COARE 3.0 bulk algorithm during the westerly wind burst. In this figure, the solar background color represents the bulk estimates, while the solid line represents the DC measurements.   The DC measurements are limited to more favorable relative wind directions to result the impact of flow distortion on our measurement. Nonetheless, the agreement between the two stress estimates is very good.   The comparison between the latent heat fluxes shows good agreement, but there are more obvious discrepancies between the estimates that require further investigations. However, it is promising to note that the closed-path IRGA deployed for this leg continued to measure fluxes while it was raining.   In fact, some of the discrepancies in the data may be driven by physical processes that occur during these rain events that are not included in the bulk algorithm.

Precipitation

The flux group spent considerable effort to determine our best estimate of precipitation during Legs 2 and 3.   This was undertaken using the seven rain gauges on board.   Three of these are manual read gauges, two are self-siphoning rain

December 7, 2011

gauges, one is optical and another is acoustic. The SCS self-siphoning gauge and the PSD optical gauge are located on the forward mast. The University of Connecticut (UConn) self-siphoning gauge is located next an OSU manual read gauge (OSUp) on the port side of the 03 deck railing. The other OSU manual read gauge (OSUs) is located on the starboard side of the 03 deck railing. The Colorado State manual read gauge (CSU) is located aft of the bridge on a railing on a platform on the 02 deck. NOAA's acoustic rain gauge (PMEL) is located on a boom mounted on the aerosol intake snorkel approximately 20ft above the 02 deck forward of the bridge. During periods of low wind, the 7 rain gauges had reasonably high agreement between their daily averages.   The PSD optical rain gauge track the other gauges very well under these conditions, but was slightly lower than these gauges by approximately 30%. However, during periods of high winds, all three manual read gauges, particularly the one aft of the bridge, and the two self-siphoning gauges appear to significantly underestimate the daily precipitation due to the rain blowing over the top of the collection reservoir, and blockage due to the ship's superstructure. The PMEL acoustic gauge was felt to over-estimate the precipitation during periods of high rain rate.   The PSD optical rain gauge continued to give reasonable results under these conditions, but the question of its calibration remained.
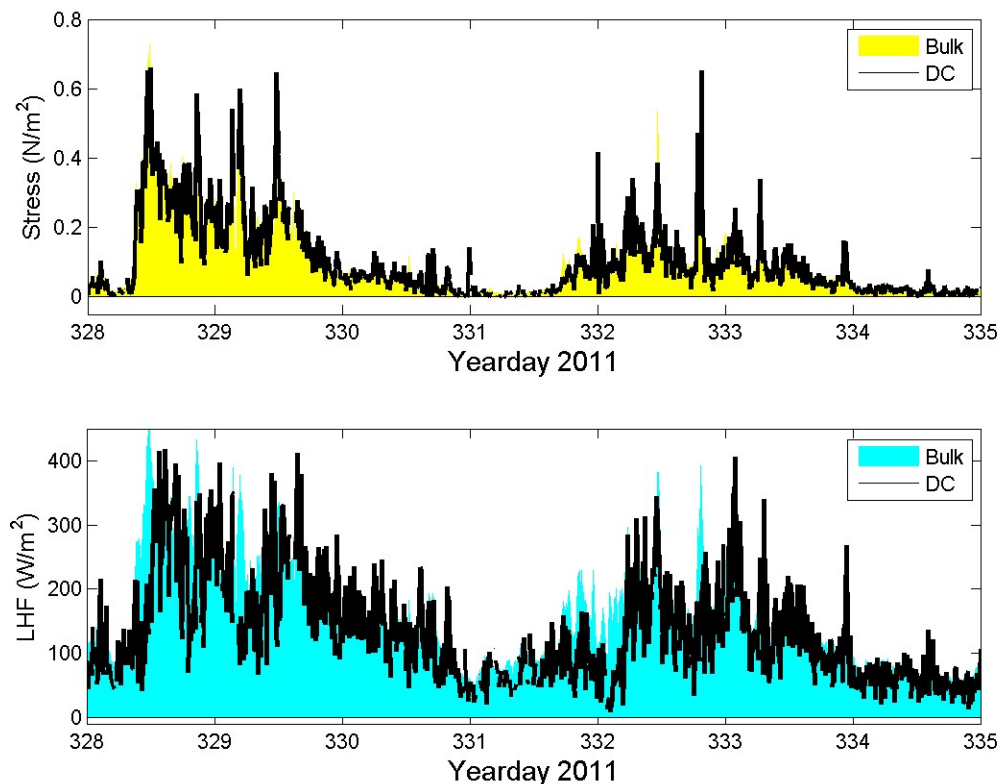
Figure 6. Time series of surface stress (top) and latent heat flux (bottom) derived from the direct covariance and bulk aerodynamic methods. The solid color is the bulk and the black line is the direct measurements.

December 7, 2011

Of particular interest was the discrepancies seen in the various gauges recorded during the 24th and 25th of November when heavy rain was observed.   Using a method that involved an examination of the heaviest rain events using the Automatic Gain Control (AGC) on the LICORs, we determined that the optical gauge is the most accurate representation of the daily rain rates after a correction factor of 1.43 was applied to its estimates of rainfall rates. Once applied, this value provided good agreement with the other gauges on low wind days when overall agreement is high as shown in Figure 4.   The optical gauge also reproduced the observed trend in the AGC data during the heavy rain and high wind events from Nov 23rd through the 25th. This correction factor also improved the overall agreement between the gauges on Leg 2. In particular, it gave good agreement between the optical rain gauge and the other sensors during the rain even at the end of Leg 2.   Therefore, the consensus of the group is that the calibrated optical gauge is the most accurate estimate of the total precipitation for the entire cruise.
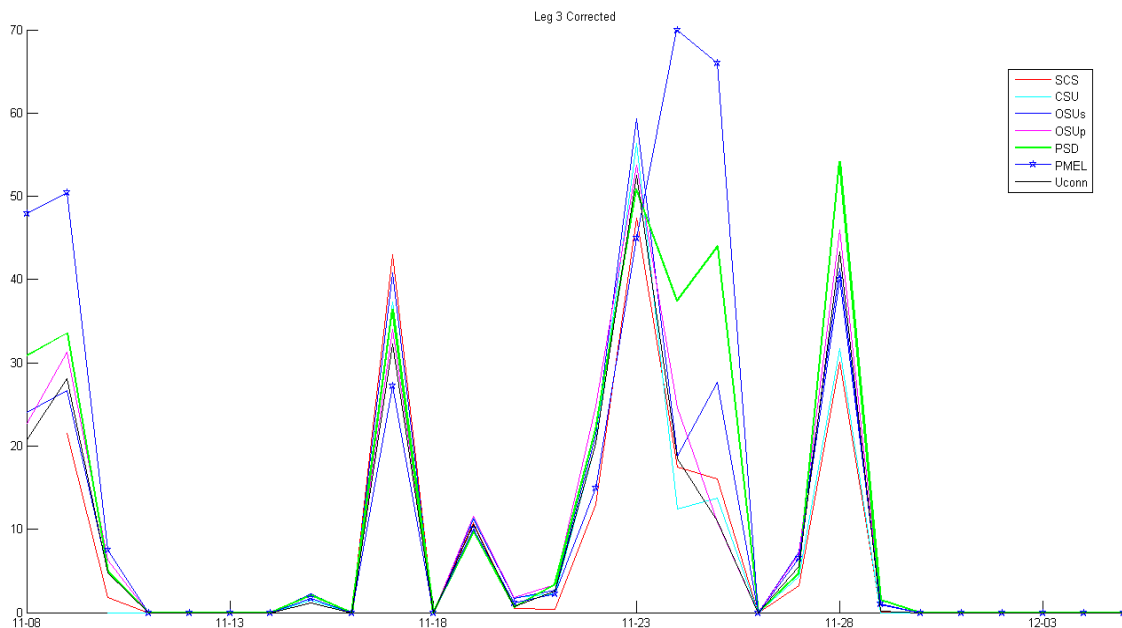
Figure 7. Daily measurements of accumulated rain measured or derived from 7 rain gauges deployed on the R/V Revelle. Our best estimate of the rainfall is given by the calibrated PSD optical rain gauge shown in green.

Mixed Layer vertical structure

The Flux group analyzed 202 soundings released from the R/V Revelle for the vertical and temporal evolution of meteorological variables from 7 November to 8 December. A preliminary Quality Control (QC) procedure was used and consisted in several steps. First, the geopotential heights computed by the radiosonde were adjusted for consistency. This was done by looking at pre-flight values and adjusting the heights to the 3-m fantail elevation where the soundings were performed. The second step was to calibrate the thermodynamic data (pressure P,

December 7, 2011

temperature T, relative humidity RH) with the highly accurate measurements made at the foremast of the ship. The average corrections obtained were: -16m for the height, -0.5°C for T, -2.2 mb for P and -2.4% for RH.   In the QC procedure, a subjective decision was also made to identify apparent problematic data points. Obvious issues were filtered out and unresolved situations were kept in the data for now. Because of questionable low altitude data points, the first 20m of each profile was also replaced by the T/RH measurements at the foremast (16m), while the 0-m value was forced to the sea surface temperature measured by the sea snake instrument. Finally after the QC-procedure, each profile was linearly interpolated to a 10m-height grid.

A time-height color contour of the local vertical potential temperature gradient is shown in Figure 5, which indicates the static stability of the atmosphere. Superimposed (dash line) is the capping inversion base height manually picked from each profiles. As expected in these situations, the lowest air is almost always superadiabatic due to the positive sea-air temperature difference. The overlying adiabatic layer represents the Convective Boundary Layer (CBL). The height of the CBL varies from ~100m up to almost 1km showing the responses of the atmosphere to air-sea exchange and mxing as well as larger-scale processes including advection of cold air masses over the ocean associated with outflows.
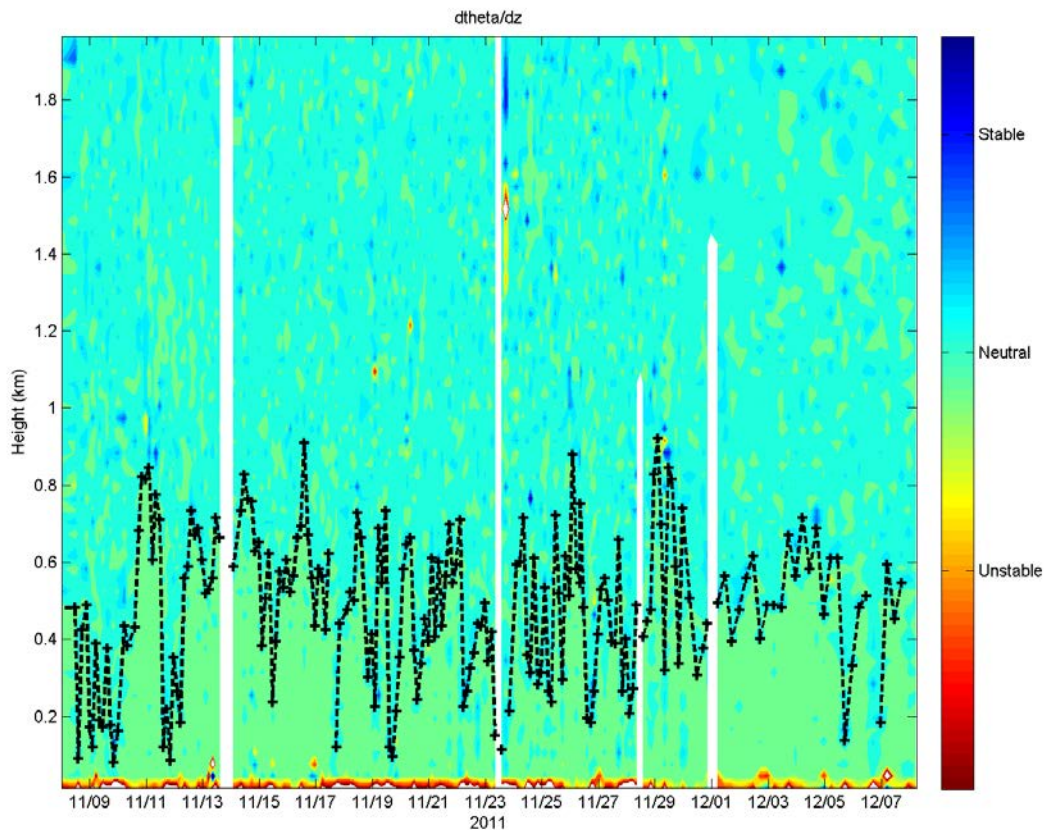

Figure 5. Time-height contour of the vertical potential temperature gradient. The black dash line indicates the inversion base height.

December 7, 2011

Remote sensors

In addition to the flux system there were 3 remote systems operated by PSD: A mechanically stabilized W-Band Doppler cloud radar, a 2-channel microwave radiometer (23 and 31 GHz) and a lidar ceilometer. The W-band radar operated continuously with no problems during Leg 3 from 7 November to 8 December. It operated in the the low mode (0-7 km) from 7 November to 1 December and the high mode (0-14 km) from 1-8 December. Both the microwave radiometer and ceilometers also performed continuously without interruption. All of the remote sensor measurements will be further post-analyzed to retrieve cloud properties (cloud droplet size, number concentration, liquid water concentration, cloud base height, etc.). As an illustration, Figure 6 shows a time-height cross section of the W-band radar reflectivity (top panel) for the whole day of 11 November. Superimposed is the cloud base from the ceilometer (stars) and the Lifting Condensation Level (LCL) determined from the radiosonde launches using the formula of Bolton (1980).   Reasonable agreement can be seen between the LCL and the first layer of clouds detected by the ceilometer. The lower panel shows the total amount of liquid water in the atmosphere measured by the 2-channel microwave radiometer. The daily summary and hourly images from the remote sensors were made available for the whole cruise.
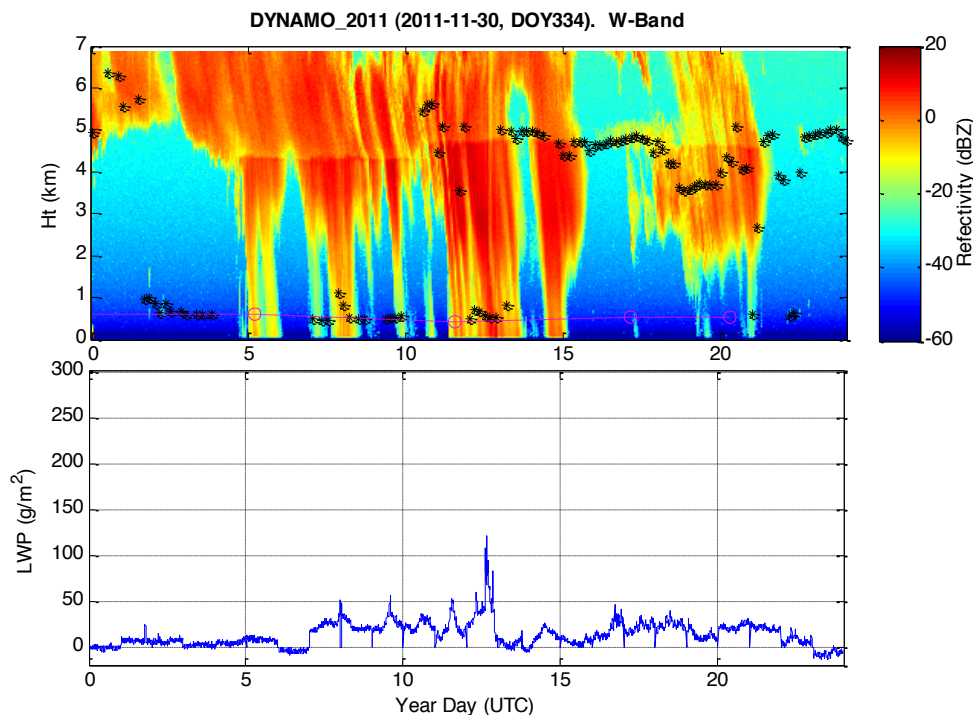

Figure 6. Top panel: time-height cross section of the Wband radar with the ceilometer cloudbase (balck stars) and the LCL estimated from the radiosondes (magenta circles). Lower panel: Integrated cloud liquid content.

December 7, 2011

CO₂ flux measurements

In addition to the suite of flux instruments, numerous atmospheric CO_2 fast-sensors were deployed during the experiment to measure the CO_2 flux. Three open-path LI-7500 sensors and a closed-path LI-7200 were collocated on the foremast during Leg 3. Another LI-7200 was installed in the PSD van using a sampling line (~30m) from the foremast to the van. Finally, a pCO_2 system from Lamont-Doherty Earth Observatory (LDEO) was used to measure the air and sea concentration of CO_2. An example of LI-7500, LI-7200 and pCO_2 measurements are shown in Figure 7. The air-sea CO_2 concentration was ~ 30ppm. Good agreement between the LI-7200 and the pCO_2 system can be seen in the CO_2 air measurement. Interestingly, the atmospheric CO_2 increased a bit for a few days during the storm events (11/22 to 11/25). We presume that this is probably associated with the variability in the origin of air mass advected past the ship. Further post-analysis will help evaluating the performance of the various instruments in such pCO_2 conditions, as well as the CO_2 variability observed during Leg 3.
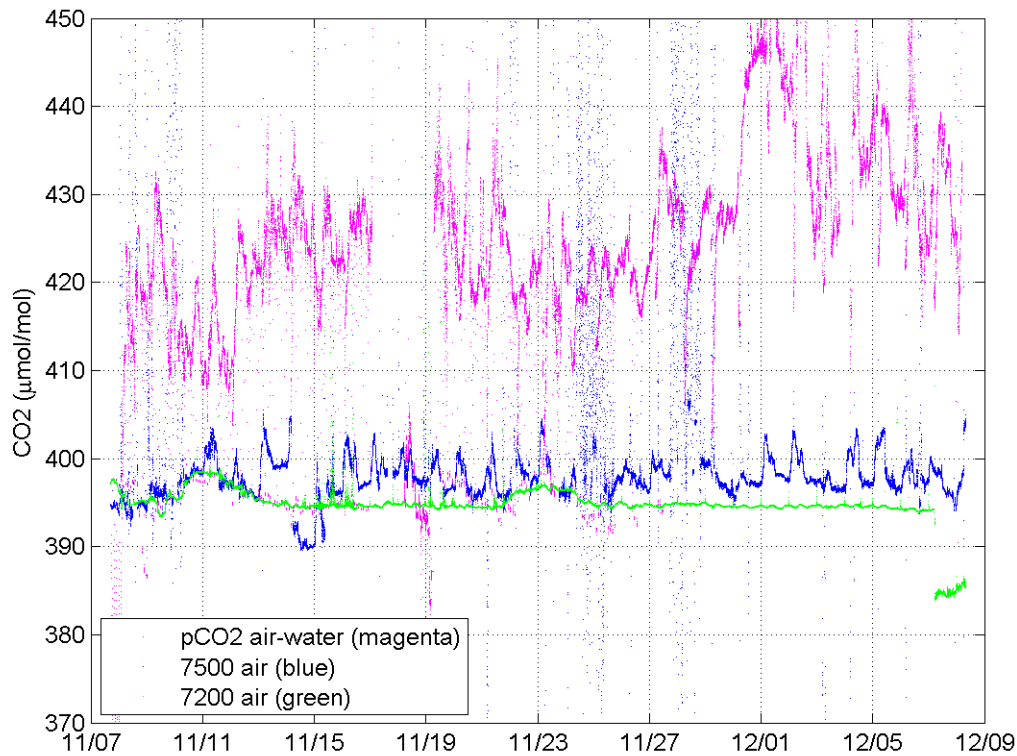

Figure 7. Time series of CO₂ air concentration from PSD LI7500 (blue) and LI7200 (green). The air-sea concentration from the pCO₂ device is also plotted (magenta). The drop in the LI7200 at the end is associated with testing of the system.

December 7, 2011

Radiosonde Group – NCAR ISS   *(Launchers:* Lou Verstraete and Timothy Lim, ISS Senior Technicians
Jonathan W. Smith, Howard University)

Number of sondes launched: Approximately 197
Start of 8 Radiosondes per day: 00 UTC, Tuesday, November 8, 2011
End of 8 Radiosondes per day: 00 UTC, Tuesday, November 29, 2011
Start of 4 Radiosondes per day: 06 UTC, Tuesday, November 29, 2011
End of all Leg 3 Radiosonde operations: 06 UTC, Thursday, December 8, 2011
There was high success rate for the number of sondes launched. Radiosonde launching operations were smooth. Squalls and gusty winds in the Active Phase of the MJO period in the third week of November made sonde launches challenging but still successful.

The next Leg of DYNAMO will want to take note of the following:
deck heating during the 06 and 09 UTC launches. Here, there could occasionally be a 10°C + temperature and /or 10% + humidity differences in the sonde versus the surface meteorology.
during convection or imminent convection, the balloon is filled with 35 cubic feet of helium as opposed to 30. This is done so the balloon would break through the freezing level in its ascent. The freezing level was often around 550 mb during Leg 3.
string line tearing during strong winds.
windy conditions on deck when the ship is moving.

December 7, 2011

Aerosols   (Derek Coffman, Kristen Schulz, Langley DeWitt)

On Leg 3 onboard the R/V Revelle we continued our continuous measurements of the chemical, physical, and optical properties of sub and supermicron aerosols in the local atmosphere. Our measurements included real-time and filter-based analysis of the aerosol chemical composition, size distributions from aitken mode to course mode aerosols, particle number concentrations, aerosol scattering and absorption, , and total mass of filter collected aerosol. We also collected meteorological data and O_3 and SO_2 gas phase measurements. With Leg 2 and Leg 3 combined we have approximately 60 days of atmospheric data at the same remote marine location.

On station during Leg 3, we observed more continental aerosol transport events than measured during Leg 2. This may be due to the changing circulation patterns associated with the MJO propagation through the Indian Ocean observed during this time period as well as the tropical cyclone occurring in the northern Indian Ocean over Thanksgiving weekend. Increased absorption and measurable elemental carbon in several aerosol events suggest an anthropogenic influence. The onset of the Indo-Asian haze, which generally occurs at the beginning of December/the dry season, may have increased the concentration of continental aerosol available for transport to the equatorial Indian Ocean.

Figure 1 shows, from the top panel to the bottom panel: O_3 and radon concentrations; submicron scattering and absorption; non-refractory submicron aerosol chemical composition; and wind speed, wind direction, and precipitation over Leg 3. Five different aerosol events have been marked.
Events 1, 2, and 3 have similar chemical compositions, exhibiting increased ammonium sulfate over the clean marine background as well as an enhanced organic aerosol signal. HYSPLIT back trajectory models confirm an aged continental air mass at the ship during these time periods, and increased radon concentrations as well as the aerosol chemical compositions during these events also supports a continental aerosol origin. Event 2 took place during the doldrums, and contained little continuous mixing down from the upper atmosphere (indicated by low O_3 during much of the doldrums), while events 1 and 3 exhibited enhanced O_3 over the background.
Event 4 , in yellow, encompasses the wind event brought on by the tropical cyclone and the passing of the active phase of the MJO over our location. Increased precipitation during this time period caused the rainout of the submicron aerosol population; however, supermicron seasalt concentrations rose sharply as the wind rose (**Figure 2**).
 HYSPLIT back trajectories suggest that Event 5 was also aged continental aerosol. The organic carbon concentration of the aerosol was not as great as in previous events. However, filter samples collected during this time period had some of the very few instances of measurable elemental carbon, and absorption also rose during this aerosol event. Methyl sulfonic acid (MSA) concentration—an indication of secondary marine aerosol—as a fraction of the total organic concentration, shown

December 7, 2011

as blue circles, also rose greatly during this time period. For the first time on station, the chlorophyll maximum was on the ocean surface during this time period. Thus,
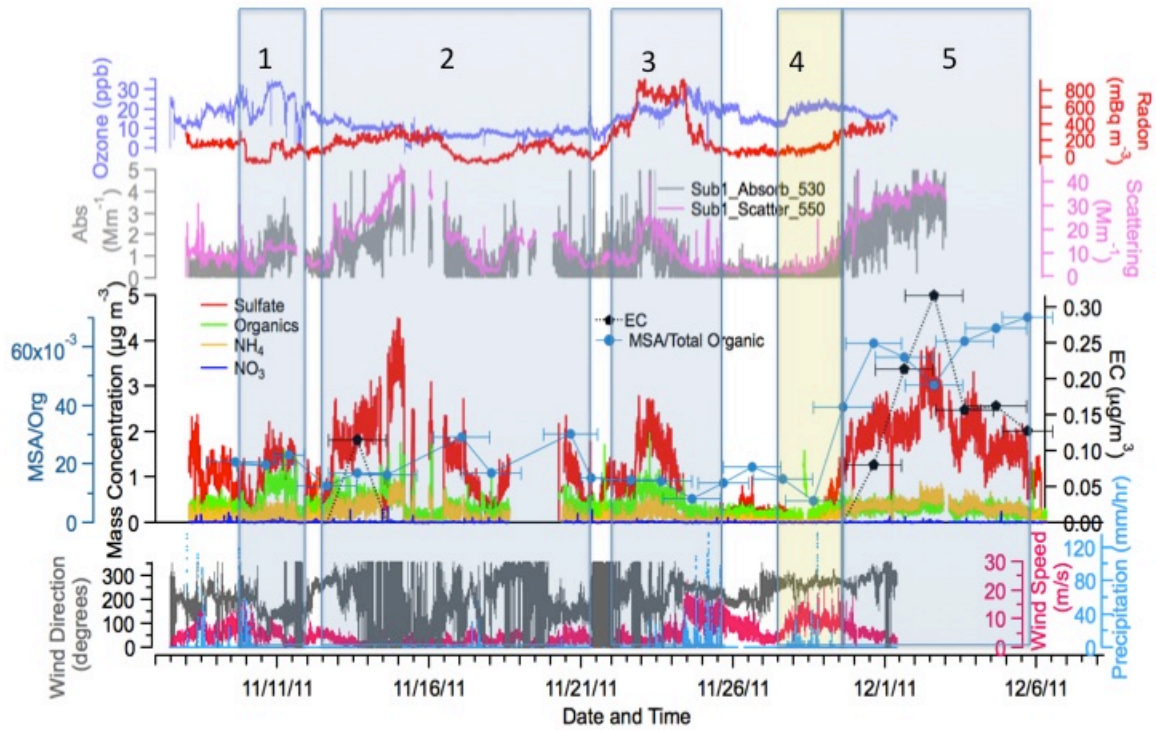
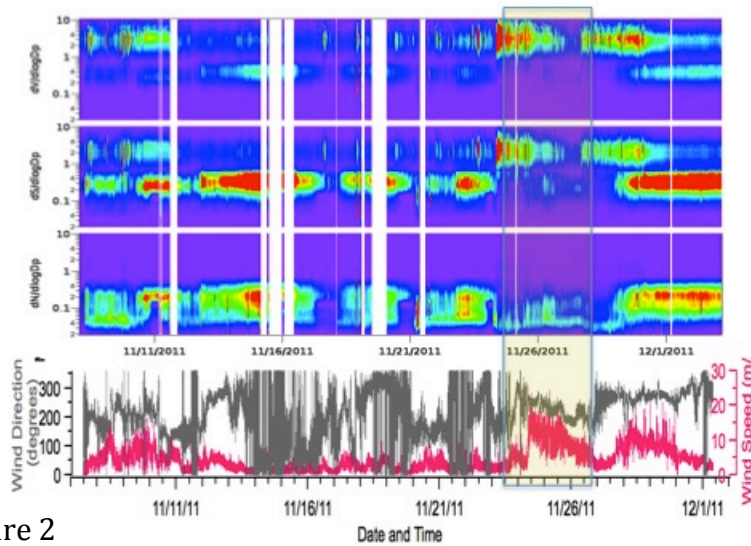event 5 may contain a mix of local marine and aged continental aerosol.
Figure 1

Figure 2

December 7, 2011

NOAA High Resolution Doppler Lidar (HRDL)   (Raul Alvarez,
                                                                                    Ann Weickmann)

Introduction

The goal of having HRDL on the RV Revelle during DYNAMO was to characterize and monitor the dynamics of the marine atmospheric boundary layer from the surface of the ocean up through cloud base or the top of the aerosol layer. This was accomplished by operating continuously during Leg 3 and performing a repeating 20-minute sequence of scans. These scans, shown in Figure 8 were designed to measure vertical profiles of the horizontal wind speed and direction, moments of the vertical wind speed, and horizontal wind variance. In addition, the scanning data can be used to visualize spatial variations and their temporal evolution in the horizontal wind field out to a range of 6-8 km and, in that mode, are useful in studying phenomena such as precipitation driven outflows. During a portion of the cruise, additional long range vertical stares were added to characterize cirrus cloud levels.
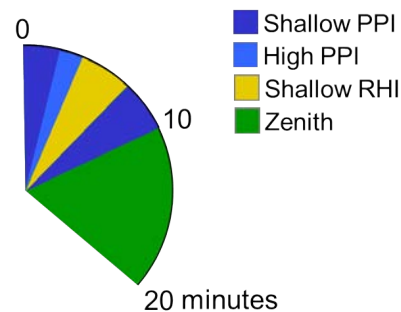

Figure 8 Twenty minute scan sequence used during DYNAMO

HRDL is a 2 micron, coherent-detection, Doppler lidar whose primary targets are atmospheric aerosol 1 micron and larger. The sensitivity of the instrument and hence its measurement range is heavily influenced by the distribution of aerosol. For typical conditions during Leg 3, HRDL could make measurements to a range of 6 km horizontally and 2-3 km vertically (typically limited by the top of the aerosol layer). Optically-thick clouds and heavy rain attenuate the signal and reduce the measurement range when present. HRDL operates with a pulse repetition frequency of 200 Hz and averages 100 pulses to form 2 Hz averaged beams of range-resolved, radial (line-of-site) wind speed and backscatter signal intensity. The along-beam resolution is matched to the length of the optical pulse which is 30 m FWHM. The diameter of the beam is approximately 0.15 m and is collimated at the output with a divergence angle of 20 μrad. The optical beam is invisible and eyesafe. HRDL is equipped with a motion compensated hemispheric scanner that is capable of maintaining pointing in the world frame with a precision of 0.5 degrees in moderate seas.

The Scan Sequence

The scan sequence shown in Figure 8 has two low-elevation-angle (1 degree) azimuthal scanning (PPI) sweeps designated as Shallow PPI. These scans have 1 degree azimuth resolution for each beam and take approximately 2 minutes to perform. They are positioned in the sequence at the beginning and middle to provide as close to a regular spacing as possible. The parameters of the azimuthal scans designated as High PPI depended on conditions and the depth of the aerosol
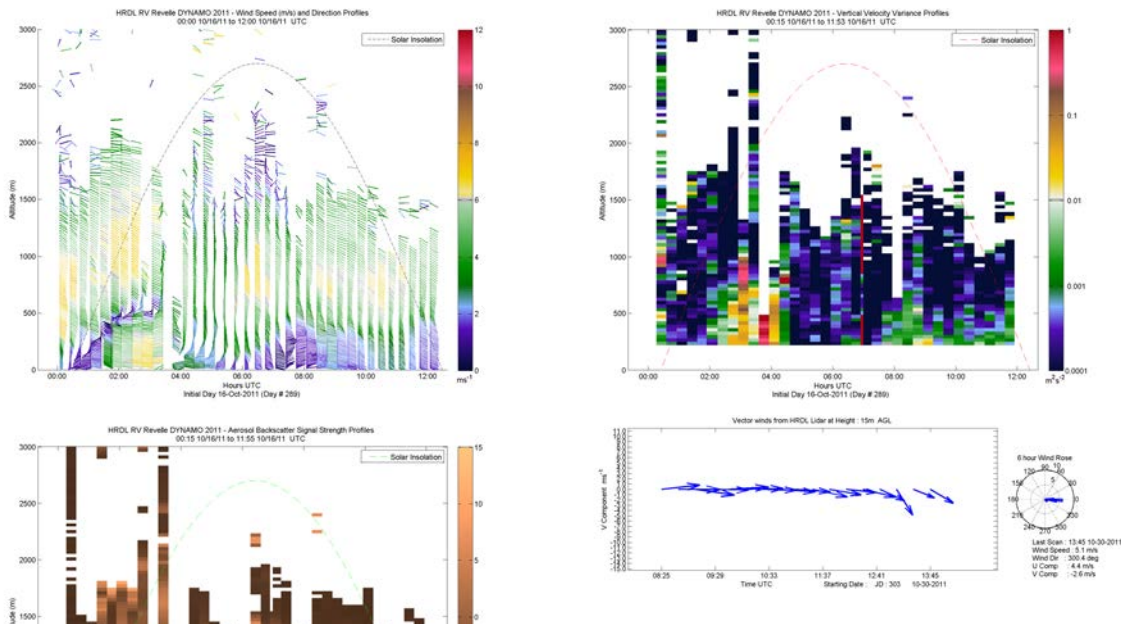
December 7, 2011

layer. Typically we operated with elevation angles of 8 and 45 degrees, but would often lower these elevation angles to fill in gaps in the vertical profiles as needed. The shallow RHI scans are elevations scans (0-30 degrees) performed at two fixed azimuth angles, typically separated by 90 degrees, one plane forward the other off the starboard side. The two-sweep pattern would be repeated 3 times giving a total of 6 sweeps, 3 in each azimuth plane. The remainder of the time (approximately 10 minutes) was spent staring vertically. For a period of three days, the first part of the vertical stare was set to our longest range setting in order to characterize cirrus clouds when present. A summary of the scans and the data products derived from them are shown in Table 1.

Table 1 Scans and associated data products

Scan	Data Product
Shallow PPI	Horizontal wind profiles, Divergence profiles, Spatial feature tracking
High PPI	Horizontal Wind Profiles, Divergence profiles
Shallow RHI	Horizontal Wind Profiles, Horizontal wind variance, Spatial feature tracking
Zenith	Moments of the vertical velocity, Cloud statistics

Realtime data products

December 7, 2011

At the end of every twenty minute scan sequence, basic data products (profiles of horizontal wind speed and direction, vertical velocity variance, aerosol backscatter signal intensity and surface wind vectors) were automatically generated and posted to a ship-based web page for on board usage. When the satellite internet connection was available, these products were also posted to a NOAA web page and were uploaded to the NCAR field catalog. When the connection was available, but limited, the results were uploaded every 4 hours. Figure 9 shows typical images of these products for a 12-hour period: Horizontal wind speed and direction, vertical velocity variance, aerosol backscatter signal strength, and surface wind vectors (for a different 6 hour period). The address of the ship-based web page is: http://hrdlpp-pc/ and the NOAA web page can be found at: http://esrl.noaa.gov/csd/lidar/dynamo.
The ship-based web page also provides a variety of other real-time products that are updated every twenty minutes: An image of every scan within the sequence, web cam images from the bore-sighted scanner and all-sky cameras, and diagnostic information including a raw, strip chart output of processed beams and a text file with current navigation and motion compensation information.
The ship-based web page also has a link to post processed results that include the most recent compilations of mean wind and boundary layer turbulence strength (vertical and horizontal velocity variance) for the given phase of the experiment (for example, the on station results shown in the results section).
Compiled Running Statistics

December 7, 2011

Figure 10 Scan chart for Leg 3 of DYNAMO. Colors represent the different scan types show the statistics and temporal coverage of the three operational periods for HRDL

HRDL operated continuously during Leg 3 with no major outages - only going offline during one brief period of heavy rain and one brief period for scanner service. Table 2 Running Statistics for Legs 1, 2, and 3. and
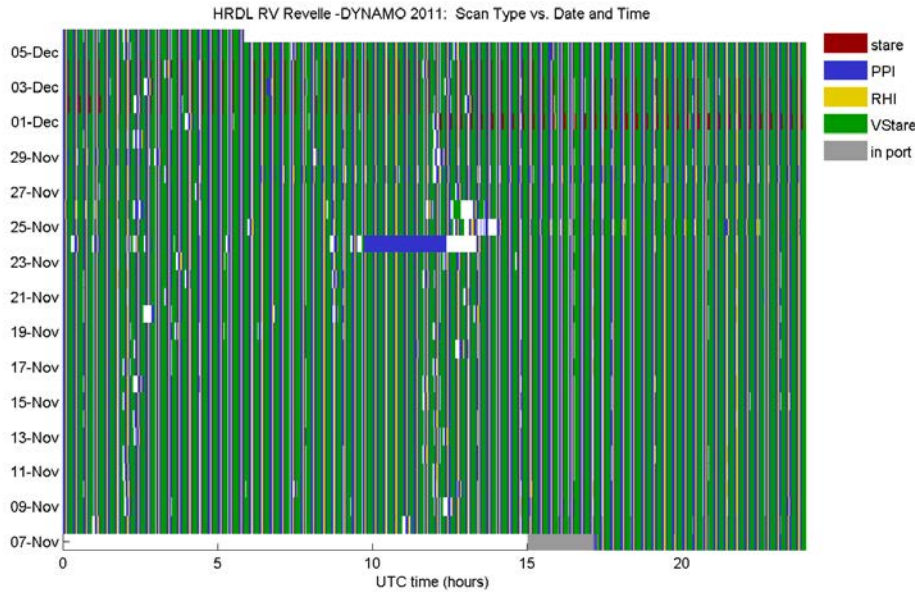
during the study. The table indicates over 650 hours of operation during Leg 3. A total 310 hours, or nearly half the time, was spent starting vertically with 95 and 250 hours spend scanning in elevation and azimuth respectively. The number of files (and hence scans) are shown in the second part of the table, broken out for each type of scan with a total of 10,300 scans for leg 3 and 29,000 scans for the study as a whole. Generating typically about 1.25 gigabytes per hour in raw data, HRDL has stored over 800 gigabytes of raw data during Leg 3 operation and nearly 2.3 terabytes for the study.

Table 2 Running Statistics for Legs 1, 2, and 3.

	Number of hours					Number of scans				
Leg	Total	zenith	30_60RHI	VAD	% data collection time	zenith	30_60RHI	1ppi	VAD	Total
1	484.2	227.4	70.6	186.2	91.7%	1576	1560	3153	1560	7849
2	690.1	328.2	103.9	258.0	96.5%	2162	2146	4320	2146	10774
3	656.8	310.0	95.4	251.5	95.9%	2112	2046	4123	2046	10327

December 7, 2011

The figure shows the temporal coverage of the scans completed during Leg 3. As
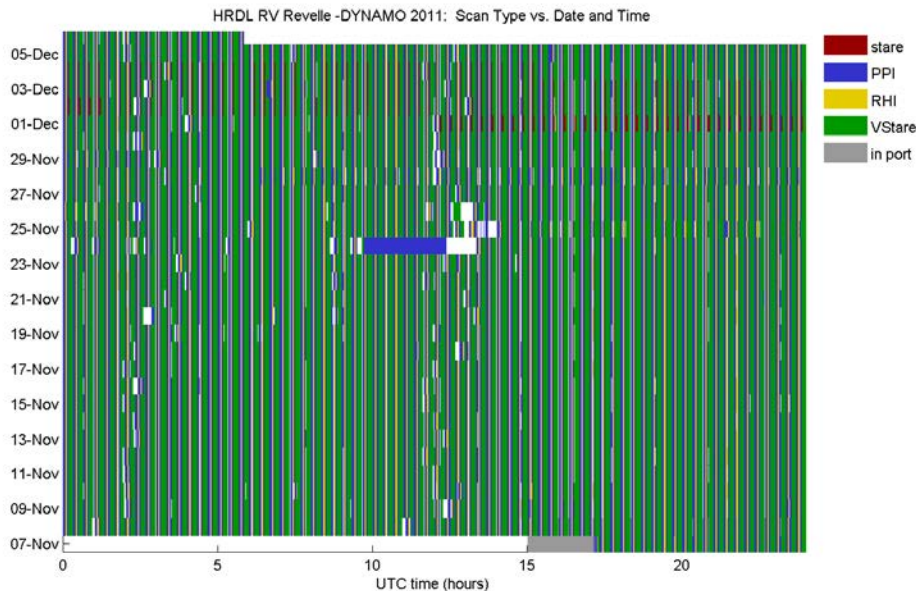

Figure 10 Scan chart for Leg 3 of DYNAMO. Colors represent the different scan types

indicated by the legend, zenith scans are green, horizontal scans blue, vertical scans yellow, and in red (added for part of Leg 3), a vertical stare with our longest measurement range for cirrus cloud characterization. The Y axis is date starting from the beginning of the leg at the bottom and progressing to the end of the leg at the top. The X axis is UTC time, 0-24 hours. Ideally, we strive for a complete, uniform pattern (to ensure even coverage and uniform sampling). The disruptions around 0200 and 1200 UTC are associated with routine maintenance performed twice a day. The blue patch on 24 Nov is a period when the scanner was having mechanical difficulty operating in high wind and rough sea conditions, and the white patch immediately following was a brief down time to repair the scanner. The coverage in Leg 3 is 95.9% and represents a well operating system with no major downtime (most of the remaining 4.1% comprises the time between the files while the scanner moves into the next starting position).

Preliminary Results

With the enormous amount of data taken during all of the cruise legs, every effort was made to analyze the data either in real time or within one day of operation, to ensure there were no subtle problems developing in the system, to monitor the conditions found on station, and to relate them to researchers on the ship and on

December 7, 2011

shore. Figure 11 shows a compilation of HRDL data products taken while on station during Leg 3. The top plot shows the insolation and rain rate during that time period. The second and third plots show the mean horizontal wind taken along the U and V directions from the surface up through 1200 meters. These results show moderate wind speeds, with nearly uniform direction as a function of height that slowly changed their direction over days. As with the previous cruise legs, there were also regular occurrences of what are believed to be precipitation driven outflows that would pass over the ship when convection was present. Leg 3 also provided a notable variation from the other cruise legs with two periods of significantly higher winds. These high winds were associated with the nearby formation of a tropical cyclone and the convective phase of the MJO occurring at nearly the same time. The white spaces in this graph occur when low clouds and heavy rain attenuated the lidar signal and are associated with the rain events shown in the top graph.

The top two panels in Figure show the distribution of the horizontal wind speed and direction as a function of height for the period of time when the ship was on station for Leg 3. Generally, the winds were out of the West at all heights, but there were periods of Southwesterly flow in the lower 700 m and periods of Northeasterly flow aloft. The wind speeds for much of Leg 3 were in the 2-4 m/s range for heights below 1000 m with a slight speed increase aloft. The exceptions, as noted above, were the two periods when the wind speeds were in excess of 20 m/s. The lower panels in that figure show a composite of the variance in the vertical (left) and horizontal (right) velocity as a function of local solar time. These results show some evidence of a diurnal pattern that peaks in the late afternoon for both the vertical and horizontal variance. The strongest variations in the horizontal variance occur both near the surface and above 500 m while the vertical velocity variance shows stronger values and variation in the lower portion of its measurement range.

Conclusion

The NOAA High Resolution Doppler Lidar operated continuously during Leg 3 of DYNAMO with a 95.9% data collection time and for all three legs of DYNAMO with a combined 95% data collection time. Leg 3 data included over 10,300 scans, and the data record for DYNAMO includes over 29,000 scans. From these scans, profiles of horizontal wind speed, moments of the vertical velocity, and backscatter signal intensity were automatically generated every 20 minutes and were made available to the ship and the wider scientific community over the internet. Initial post processed results show interesting features in the horizontal wind field distribution and diurnal patterns in the vertical and horizontal variances. Precipitation driven outflows were encountered with great regularity and a couple of high-wind events were observed. Efforts are underway to use HRDL data together with other measurements made on the ship to characterize these varied events and to examine any linkages with ocean mixing.

December 7, 2011

NOAA Doppler Lidar R/V Revelle DYNAMO   VAD and Zenith Results
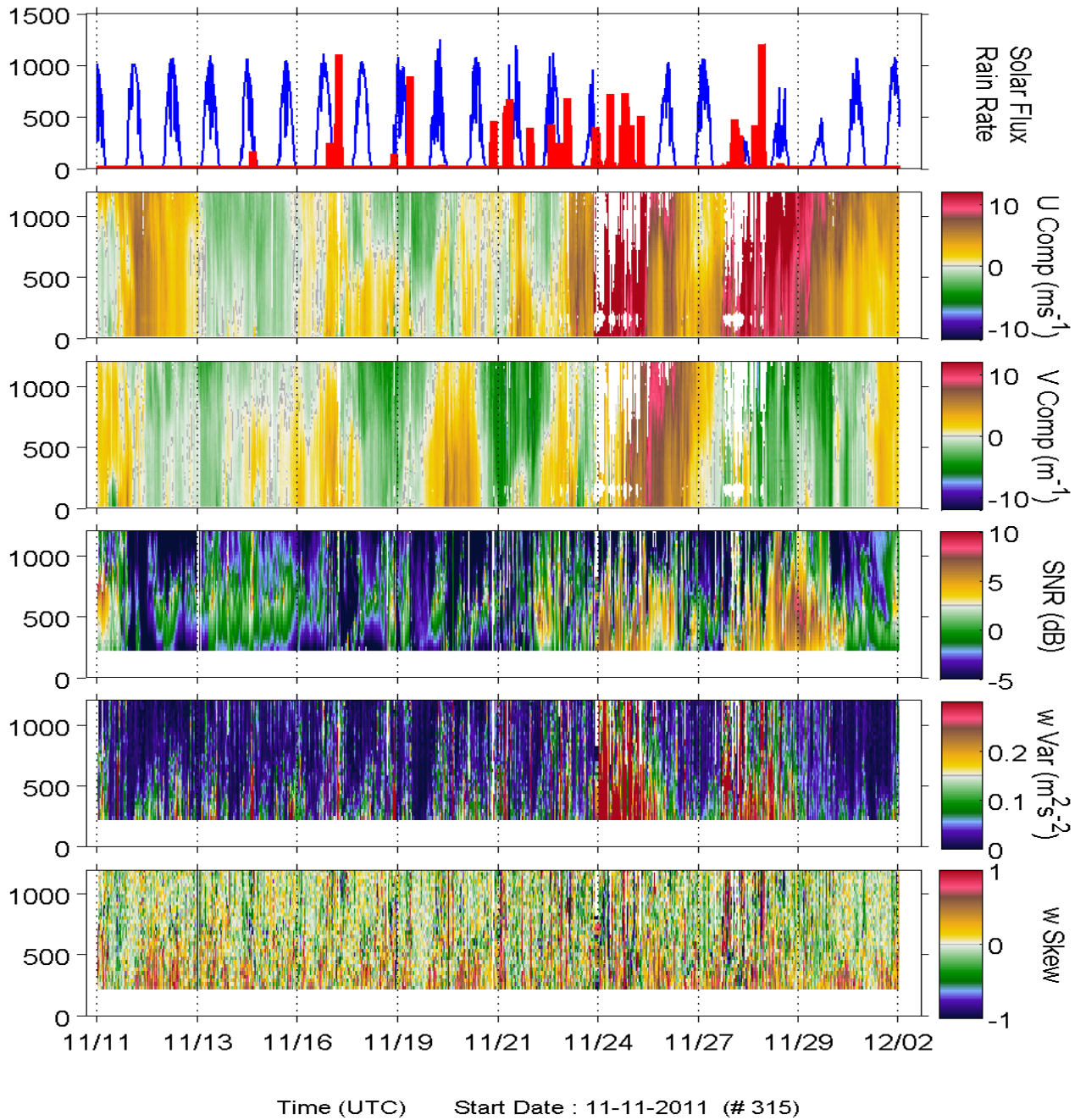

Figure 11 Compilation of results from HRDL while on station during Leg 3. The plots are of solar Insolation and rain rate, U and V components of the mean wind, Backscatter intensity signal, and variance and skewness of the vertical velocity distribution for data
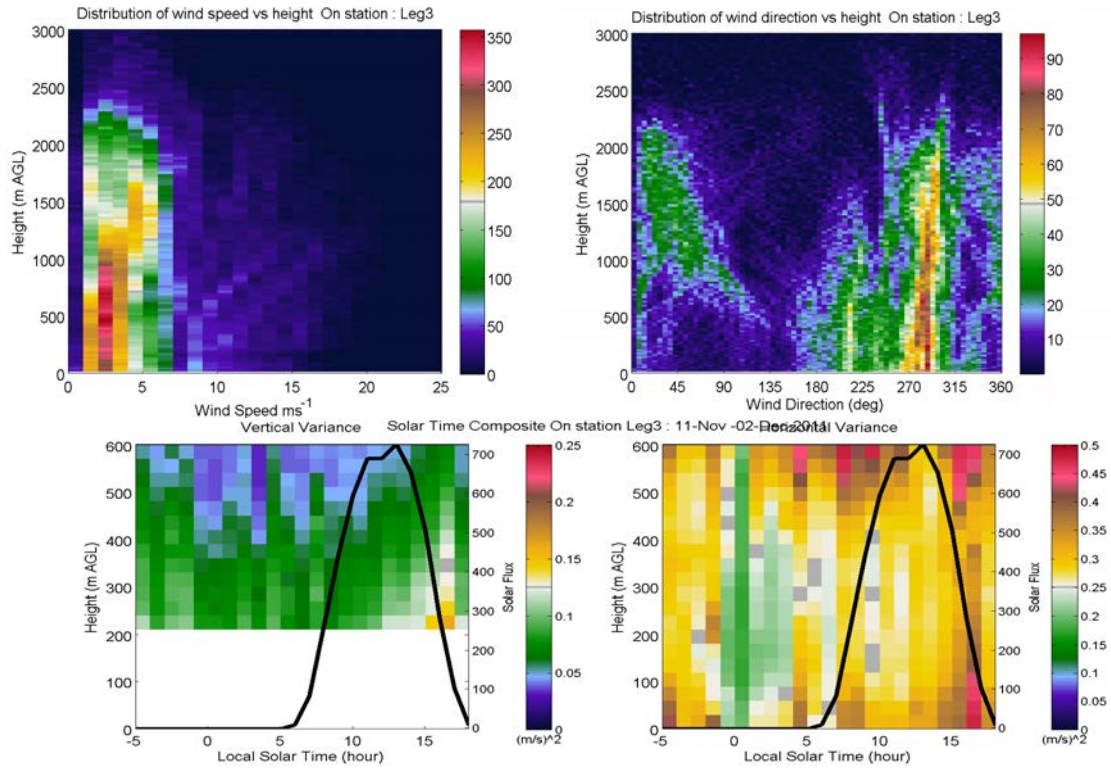
December 7, 2011

Figure 5 Distributions of wind speed and direction vs height (top) and (bot) Vertical and Horizontal velocity variance composited as a function of local solar time.

December 7, 2011

TOGA C-Band Doppler Radar (OWEN SHIEH, *University of Hawaii*
ELIZABETH THOMPSON, Colorado State
MICHAEL WATSON NASA Wallops Flight Facility)

The NASA TOGA C-band Doppler radar began collecting data at 1740 UTC on 7 November, running nearly continuously until 0830 UTC on 8 December. Full 360-degree volume scans with 150 km radial range were scheduled at 10-minute intervals, each requiring almost 9 minutes to complete. This provided approximately 1 minute of time for vertical cross-sections (Range-Height Indicator scans, RHIs), usually consisting of 5 azimuthal angles with 1- or 2-degree spacing. A single low-level (0.8-degree elevation angle) scan was completed to a range of 300 km at :29 and :59 minutes past the hour instead of RHIs. This scan was made available on CSU's DYNAMO website (http://radarmet.atmos.colostate.edu/dynamo) and the DYNAMO field catalog. As with Cruise 2, nearly 700 hours of data were collected from the TOGA radar, resulting in approximately 3,500 full volume scans and roughly 13,000 RHIs, providing an extensive dataset for computing echo statistics and for determining horizontal and vertical characteristics of precipitation.

Several additional radar products were created during Cruise 2, which were continued throughout Cruise 3. These included 10-minute updates of echo-top height across the 150-km radius domain and 24-hour accumulated rainfall at each range bin. While these provided only rough estimates due to the extensive quality-control effort that will be required to eliminate non-meteorological echo, they proved to be useful tools for describing the relative day-to-day trends of precipitating features. To this end, an algorithm was developed during Cruise 3 to qualitatively estimate daily and hourly radar-integrated rainfall for any point within the 150 km TOGA radar domain. Despite the "cone of silence," whereby the radar's limited elevation angles prevented the sensing of atmospheric scatterers directly above the ship, the radar-integrated daily rainfall amounts approximately correlated with the aggregate average of daily ship rain gauge measurements. A preliminary spectral analysis of radar-integrated hourly rainfall indicated a semi-diurnal cycle in convective activity, possibly associated with the afternoon maximum in daytime heating and instability due to the early morning deviation from radiative-convective equilibrium. Radar data must be quality-controlled before any quantitative rainfall statistics can be produced.

Throughout Cruise 3, both stratiform and convective precipitation types were observed. A broad spectrum of convection ranged from shallow, short-lived, isolated cells to large mesoscale convective systems (MCSs) with embedded regions of stronger convection extending on average to 14-16 km in height. The highest echo tops reached approximately 18 km. The modes of echo top heights observed during this cruise support TOGA-COARE observations of a trimodal distribution of clouds over the tropical oceans: cumulonimbus extending past 12 km to the tropopause, cumulus congestus reaching 7-9 km, and trade wind cumulus in the lower 4 km of the atmosphere. Stratiform precipitation frequently displayed evidence of melting ice species near the 0ºC level, which resulted in a local,

December 7, 2011

horizontally-oriented enhancement of radar reflectivity known as the bright band (Figure 1). The maximum reflectivity value captured in RHI scans during this cruise was 59 dBZ. Finally, cold outflow boundaries were observed to propagate away from mature convective elements during this cruise, sometimes acting to initiate or organize new convection. These fine lines were most often observed overnight and seemed to persist for a very long time, well after the original convection had dissipated.

The TOGA radar was properly positioned to continuously sample convection before, during, and after the active phase of the MJO. As illustrated in the preliminary daily and hourly precipitation time series (Figure 2), there was a step-function increase in rainfall within the TOGA radar domain associated with the rapid arrival of the MJO around Julian Day (JD) 320. Low-level westerly winds became stronger and more persistent near the *R/V Roger Revelle*, as opposed to the light and variable low-level winds observed during the suppressed phase (JD 315-320). This directional wind shear seemed to contribute to the development and maintenance of long-lived, organized MCSs, including strong squall lines with surface wind gusts over 40 kts and rough seas (Figure 3). Interaction between preexisting MJO convection and the nearby development of Tropical Cyclone 05A caused a further enhancement of rainfall. Once the tropical cyclone disassociated from the active MJO convective envelope, another suppressed MJO phase passed through our domain. Subsidence and dry mid-level air with dew point depressions exceeding 20°C inhibited deep, widespread convection until approximately JD 340 as the *R/V Roger Revelle* sailed back to Thailand.
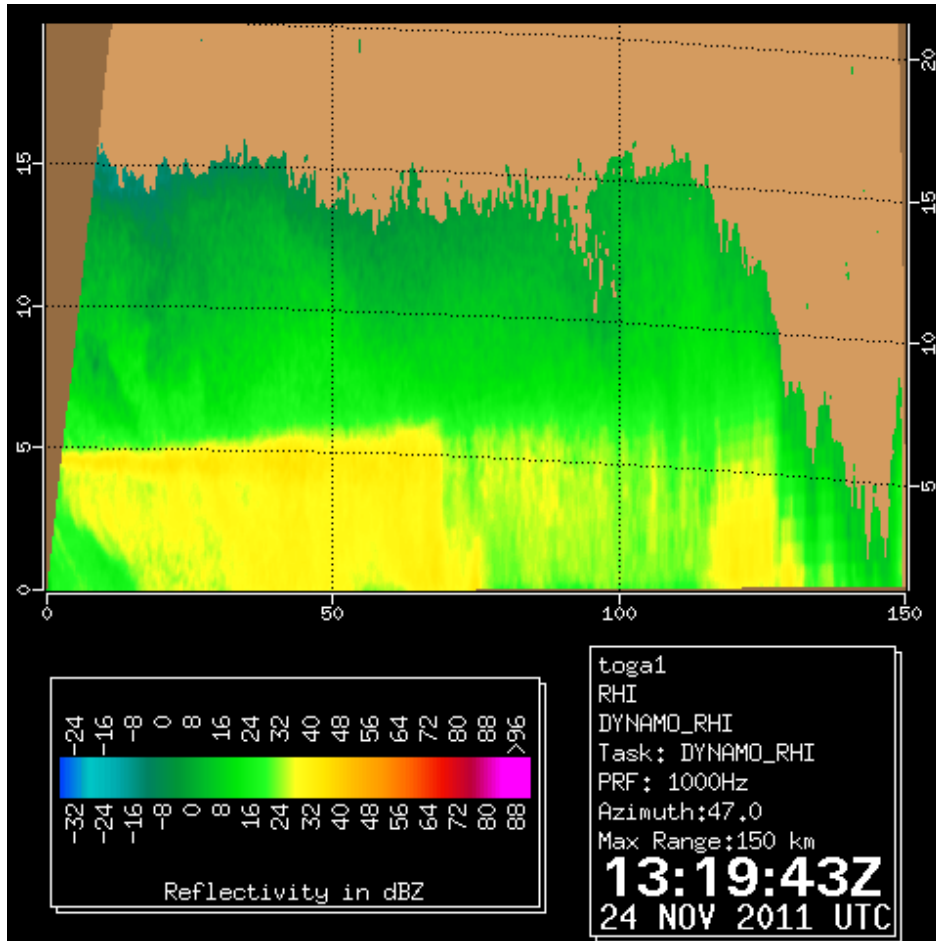
December 7, 2011

Figure 1: Typical Range-Height Indicator (RHI) radar reflectivity scan into stratiform precipitation at 1339 UTC on 24 Nov 2011. X- and Y-axes indicate horizontal and vertical distance [km] away from the radar, respectively. Radar indicated bright band is evident near the environmental freezing level ~5 km.
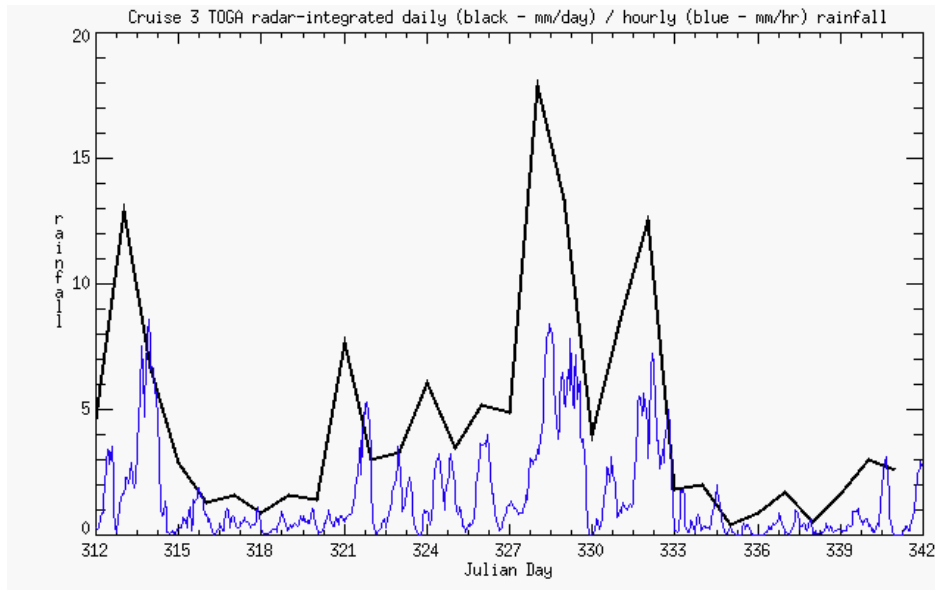
December 7, 2011

Figure 2: Daily (black [mm/day]) and hourly (blue [mm/hour]) radar-integrated rainfall within the 150 km TOGA radar domain during Cruise 3. The *R/V Roger Revelle* was on station between Julian Days 316-336, and otherwise in transit to/from Thailand. Reflectivity values from the entire domain were summed, converted to rainfall rate [mm/hr] using a Z-R relationship, and then divided by the total domain area to produce a point average rainfall amount. Integrated rainfall was calculated between 0000-2359 UTC for each day.
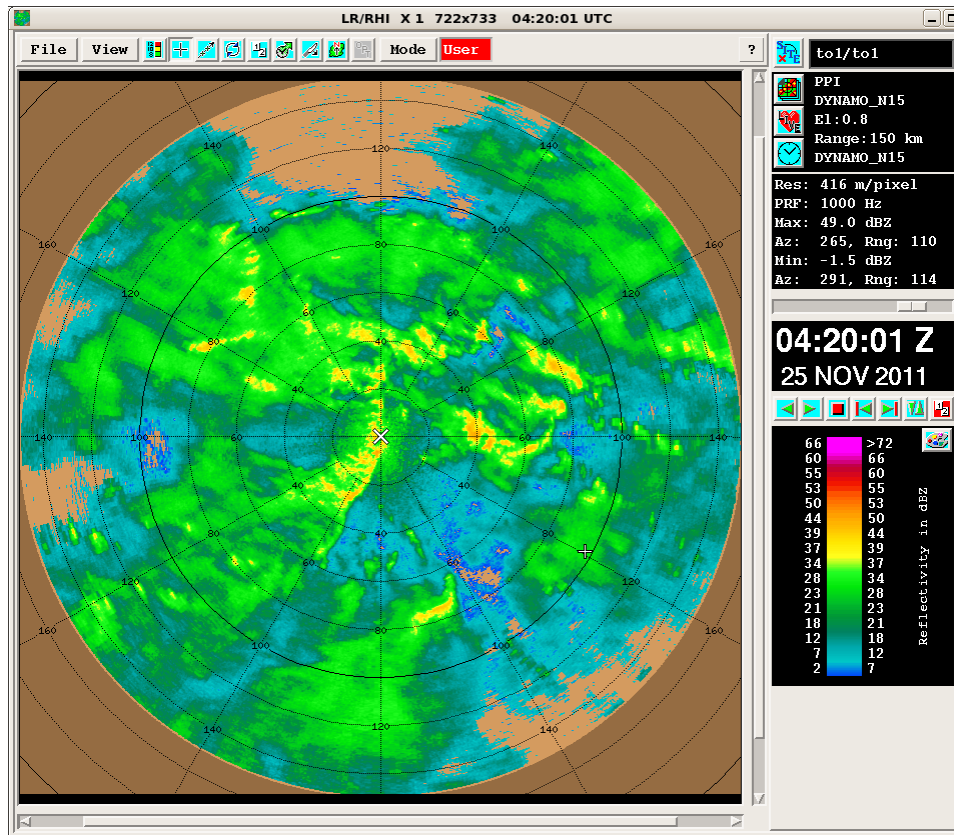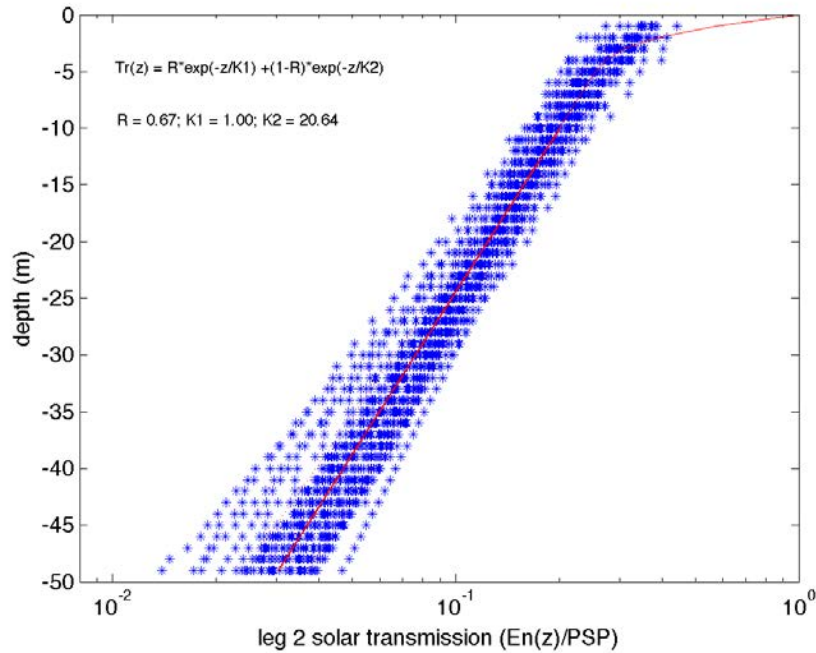
December 7, 2011

Figure 3: Low-level (0.8 degree elevation angle) Plan Position Indicator (PPI) radar reflectivity scan at 0420 UTC on 25 November 2011. Range rings indicate horizontal distance [km] away from radar. A fast moving, intense squall line passed over the *R/V Roger Revelle* at this time. Rain continued for several hours afterward.

December 7, 2011

Optics   (KG Fairbairn)

We completed 32 days of optics casts to 50 meters, 3 casts per day at 0900, 1200, and 1500 local time. The 0900 cast on November 25 was canceled due to high sea state and ship maneuvering. Water samples from the CTD were taken at the surface and at the Chlorophyll maximum which varied from 35 meters to 80 meters. The samples will be analyzed at a later date.

December 7, 2011

Ocean Mixing   (J.N. Moum, W.D. Smyth, A. Perlin, M. Neeley-Brown, R. Kreth,
L. Neeley-Brown, R. Brown, E. McHugh, A. Moulin, J. Osborne)

The Ocean Mixing Group from Oregon State University was responsible for sonar measurements of ocean current profiles, high-frequency measurements of acoustic backscatter, turbulence/CTD profiling measurements, 22 drifter launches and near-surface CTD measurements using bow chain-mounted sensors (7 Seabird microcats + 8 fast thermistors in the upper 10 m). Over DYNAMO Legs 2,3, 46 days of station profiling was conducted, resulting in 7239 turbulence/CTD profiles to 300 m nominal depth. Periods of continued station profiling were
Leg 2: 14:00 04 October 2011 – 03:00 28 October 2011
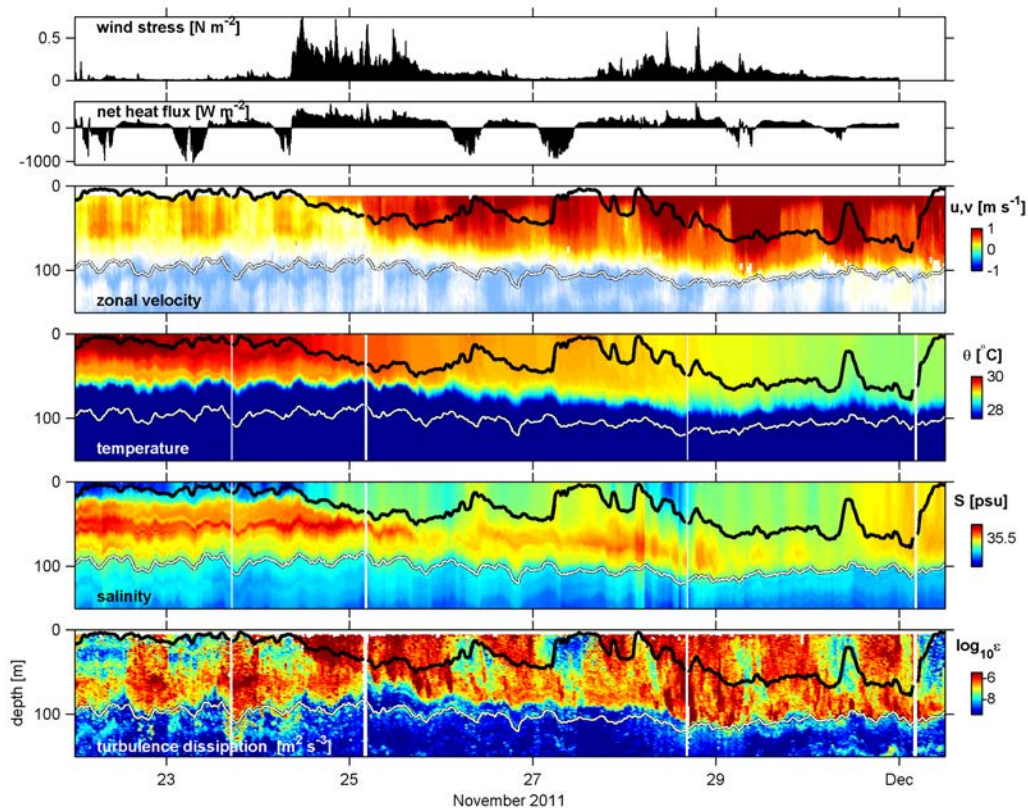Leg 3: 06:00 11 November 2011 – 10:00 02 December 2011

Figure O1 – Summary time series of the passage of the cyclone-assisted MJO wind burst past R/V Revelle on 24 November 2011. The wind stress appears as a step-function change from <0.05 Pa to > 0.5 Pa in a few minutes. Net surface cooling lasted for more than 1 day, a rarity at the equator. The eastward surface current (the Wyrtki Jet) accelerated from < 0.5 m/s in about 1 day, deepening with time. The mixed layer is indicated by the black line, the potential density surface 24.75 by the white line. Mixed layer cooling was driven by combined atmospheric and subsurface cooling. Salinification of the surface was driven by excess of subsurface mixing over precipitation. Intense turbulence (lower panel) caused directly by surface forcing on 24 November was followed by shear-driven mixing at the base of the Jet (to 100 m).

December 7, 2011

The highlight of Leg 3 was the observation of a complete MJO cycle including a cyclone-assisted MJO wind burst at Revelle. Excess surface heating over the sum of atmospheric + subsurface cooling caused increased sea surface temperatures prior to 24 November during the suppressed phase of the MJO. On 24 November, the arrival of MJO-related winds/convection in the west juxtaposed with Tropical Cyclone 05-A from the NE resulted in a rapid increase of wind stress at Revelle from near-zero to 0.35 Pa sustained over the next 24 h. The step function in wind stress, the net surface heating and the ocean's response are illustrated in Figure O1. Despite significant precipitation, subsurface mixing caused surface salinity to increase rather than decrease. Combined atmospheric cooling of the ocean from above and ocean cooling from below caused rapid sea surface cooling. And in perhaps the simplest dynamical air-sea interaction response possible, the surface Wyrtki Jet was accelerated from <1 kt to > 2.5 kts in the period of a day by the excess of wind stress over turbulence friction at the base of the Jet. The Jet response is seen in the time series in Figure O1. The large-scale Jet response is seen in the pair of zonal transects made before and after the MJO wind burst (Figure O2).
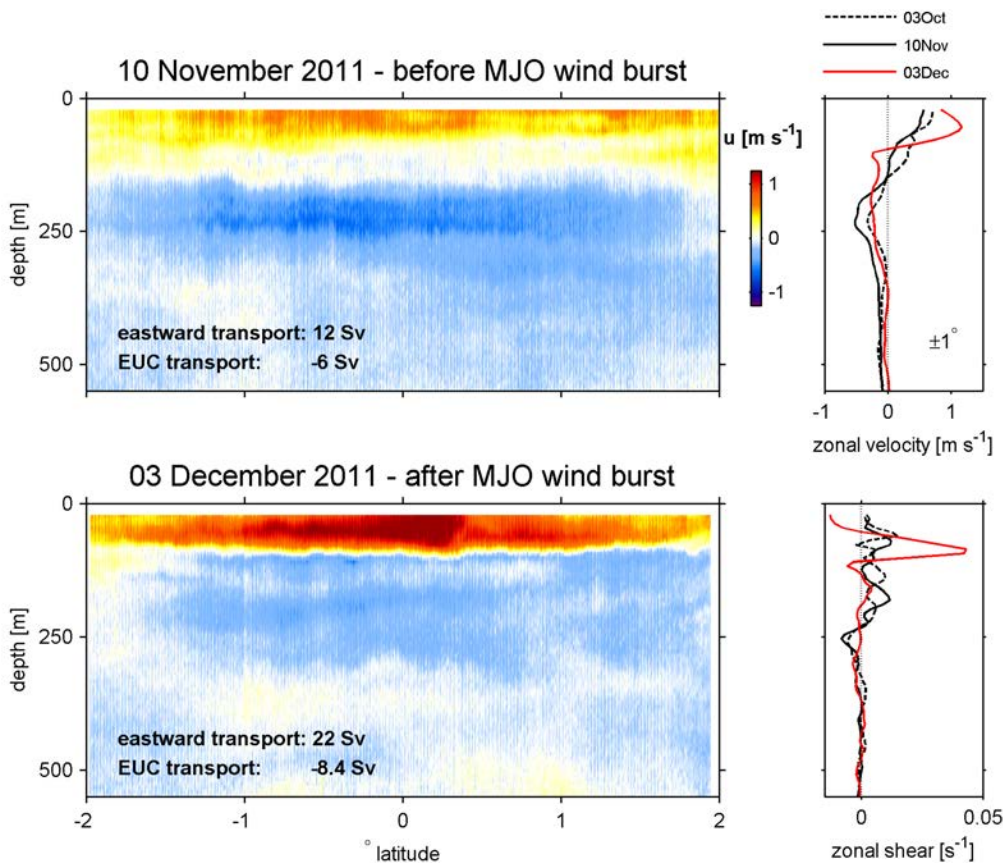

Figure O2 – Cross-equatorial structure of the Wyrtki Jet before and after passage of the cyclone-assisted MJO wind burst. Images are zonal currents between 2S and 2N along 080 30.0'E. Eastward transport increased by a factor of 2 following the wind burst. This is equivalent to a quadrupling of surface ocean kinetic energy. Mean vertical profiles of zonal currents (upper right) and current shear (lower right) provide a direct comparison of the intensification between 1S and 1N.

December 7, 2011

Drifter tracks (Figure O3) to 02Dec indicate a range of behavior that will be interesting to follow over the next few months.
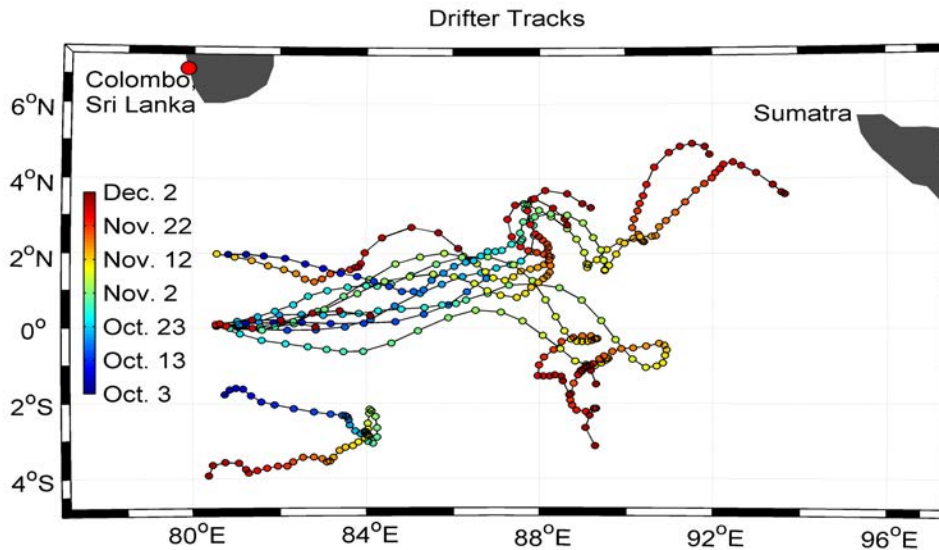

Figure O3 – Drifter tracks (to 02Dec2011) from drifters released on DYNAMO Legs 2,3.

Zonal velocities in the upper 600m show three main features (Figure O4). In the upper 100m is the east-flowing Wyrtki jet. Between this and 300m is the equatorial undercurrent. Below 300m is a field of oscillatory motions with distinct upward phase propagation. While the dataset does not encompass a full period, it it allows some inferences about the dominant scales of this propagating signal.

The sloping line defines upward phase propagation at a rate of 5.7m/day (estimated graphically from the slope of the isotachs). We cannot measure the period or the vertical wavelength, but this phase velocity gives us their ratio. We will consider two possible periods and their corresponding wavelengths. Eastward velocity fluctuations appear at the domain bottom around day 325. The previous appearance of westward fluctuations is not resolved, but it may have occurred within a few days before the observation period began at day 280. We can therefore take 325-280=55 days as a lower bound for the half-period. Equivalently, the period is greater than 110 days.

An intriguing possibility that these observations do not rule out (though additional data may) is that the period is semiannual, corresponding to the monsoon cycle and the Wyrtki jet. The corresponding vertical wavelength is 1000m. Kelvin waves of this period were observed in this region by Luyten & Roemmich (1982), although they observed a longer vertical scale.
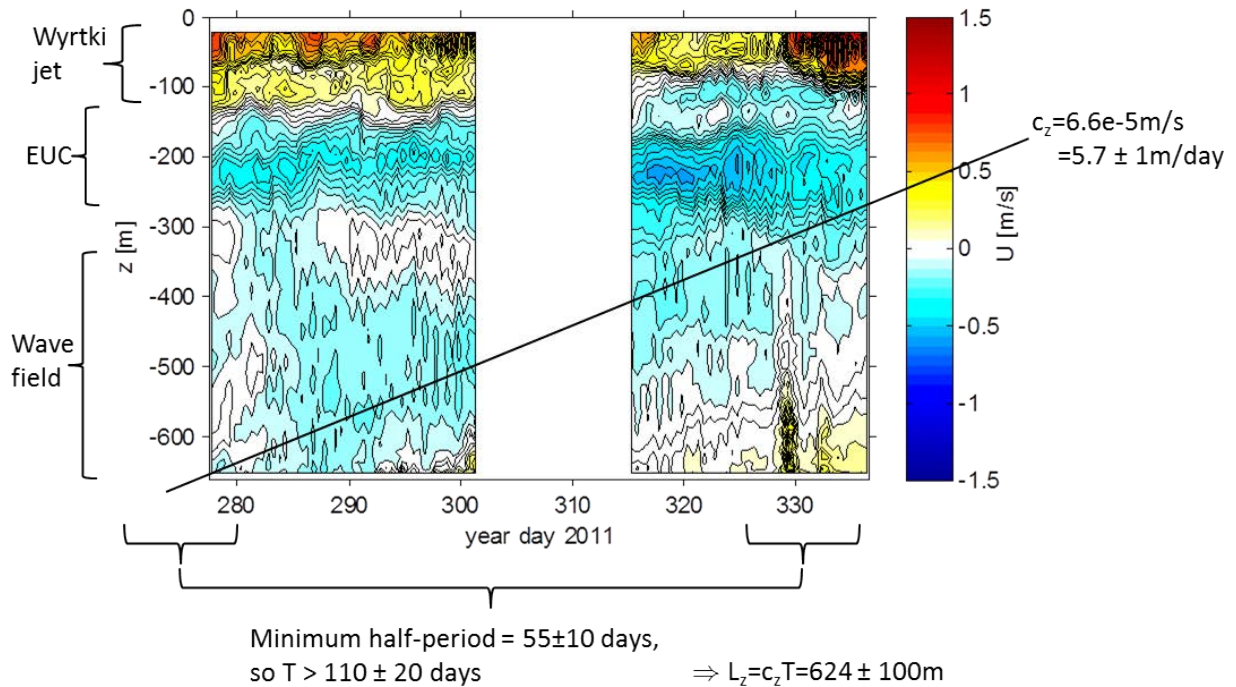
December 7, 2011

Figure O4 – Zonal velocities upper 600 m at 0, 80.5E, 03Oct - 03Dec 2011.

In summary, we hypothesize that **these fluctuations represent a semiannual Kelvin wave forced by fluctuations in the Wyrtki jet.**

Zonal and meridional transects performed during leg 3 are now being analyzed to test this hypothesis in the context of the linear theory for free, equatorially trapped waves. Preliminary results indicate that the wave has a critical level within the Wyrtki jet, and therefore that strong interaction between the wave field and the jet is possible. Extension of the observations in upcoming legs of Dynamo will greatly facilitate these analyses.

The observations also reveal a 21-day fluctuation in meridional velocity that may be identifiable as a Yanai wave, as well as numerous fluctuations of shorter period.

December 7, 2011

Event Log

2315z 11/07/11 04 52.87N. 089 29.06E. WX 1 deployed TD
1118z 11/08/11 04 07.05N. 087 06.02E. WX 2 balloon deployed EW
1414z 11/08/11 03 56.78N. 086 33.94E. WX Balloon 3 deployed MS
1715z 11/08/11 03 45.79N. 085 59.71E. WX Balloon 4 deployed MS
2057z 11/07/11 05 02.49N. 089 59.17E. WX Ballon 5 deployed MT
2317z 11/07/11 04 52.73N. 089 28.61E. WX Balloon 6 deployed TD
2348z 11/08/11 03 22.10N. 084 45.83E. WS Balloon 6 deployed again TD
0218z 11/09/11 03 13.25N. 084 18.28E. WX Balloon 7 deployed MS
0516z 11/08/11 04 28.28N. 088 12.28E. WX Balloon 8 deployed MS
0818z 11/09/11 02 51.44N. 083 10.28E. WX Balloon 9 deployed MT
1113z 11/09/11 02 41.06N. 082 37.90E. WX Balloon 10 deployed MS
1444z 11/09/11 02 28.90N. 082 00.00E. WX Balloon 11 deployed MS
1715z 11/09/11 02 19.92N. 081 32.05E. WX Balloon 12 deployed MS
2016z 11/09/11 02 09.35N. 080 59.14E. WX Balloon 13 deployed MT
2255z 11/09/11 01 59.80N. 080 30.04E. Drifter 1 deployed TD
2257z 11/09/11 01 59.39N. 080 30.01E. XBT Deployed TD
2315z 11/09/11 01 55.65N. 080 29.99E. WX Balloon 14 Deployed TD
2340z 11/08/11 03 22.57N. 084 47.30E. XBT Deployed TD
2345z 11/08/11 03 22.29N. 084 46.38E. WX Balloon 15 deployed TD
0013z 11/09/11 03 20.63N. 084 41.21E. XBT Deployed TD
0130z 11/10/11 01 27.75N. 080 30.00E. XBT Deployed TD
0208z 11/10/11 01 19.81N. 080 29.99E. XBT deployed MS
0215z 11/10/11 01 18.34N. 080 30.00E. WX Balloon 16 deployed MS
0248z 11/10/11 01 11.44N. 080 30.01E. XBT deployed MS
0325z 11/10/11 01 03.72N. 080 30.00E. XBT deployed MS
0405z 11/10/11 00 55.62N. 080 30.01E. XBT deployed MS
0444z 11/10/11 00 47.72N. 080 29.99E. XBT deployed MS
0522z 11/10/11 00 40.11N. 080 30.00E. WX Balloon 17 deployed MS
0525z 11/09/11 03 01.82N. 083 42.59E. XBT deployed MS
0604z 11/10/11 00 31.82N. 080 30.00E. XBT deployed MT
0644z 11/10/11 00 23.74N. 080 30.01E. XBT deployed MT
0723z 11/10/11 00 15.85N. 080 29.99E. XBT deployed MT
0802z 11/10/11 00 07.98N. 080 29.99E. XBT deployed MT
0805z 11/10/11 00 07.38N. 080 30.01E. WX Balloon 18 deployed MT
0842z 11/10/11 00 00.15S. 080 29.99E. XBT deployed MT
0922z 11/10/11 00 08.25S. 080 30.01E. XBT deployed MT
1003z 11/10/11 00 16.34S. 080 29.99E. XBT deployed EW
1044z 11/10/11 00 24.51S. 080 30.00E. XBT deployed EW
1113z 11/10/11 00 30.32S. 080 30.02E. WX Balloon 19 deployed MS
1123z 11/10/11 00 32.32S. 080 29.99E. XBT deployed MS
1242z 11/10/11 00 48.26S. 080 30.00E. XBT deployed EW
1323z 11/10/11 00 56.60S. 080 30.01E. XBT deployed EW
1401z 11/10/11 01 04.42S. 080 30.02E. XBT deployed MS

December 7, 2011

1417z 11/10/11 01 07.69S. 080 29.99E. WX Balloon 20 deployed MS
1440z 11/10/11 01 12.39S. 080 29.98E. XBT deployed MS
1519z 11/10/11 01 20.30S. 080 29.99E. XBT deployed MS
1559z 11/10/11 01 28.31S. 080 30.01E. XBT deployed MS
1639z 11/09/11 02 22.02N. 081 38.54E. XBT deployed MS
1727z 11/10/11 01 45.99S. 080 30.02E. XBT deployed MS
1759z 11/10/11 01 52.42S. 080 30.01E. XBT deployed MT
1837z 11/10/11 02 00.09S. 080 29.99E. XBT deployed MT
1840z 11/10/11 02 00.70S. 080 29.92E. Drifter deployed MT
2013z 11/10/11 01 44.60S. 080 29.79E. WB Balloon 20 deployed MT
2342z 11/10/11 00 58.91S. 080 30.96E. WX Balloon #22 Deployed TD
0219z 11/11/11 00 25.06S. 080 31.79E. WX Balloon 23 deployed MS
0455z 11/11/11 00 04.40N. 080 32.57E. Drifter 82309 deployed MS
0456z 11/11/11 00 04.40N. 080 32.57E. CTD 1 deployed MS
0519z 11/11/11 00 04.42N. 080 32.56E. CTD 1 @ depth 1000m MS
0541z 11/11/11 00 04.43N. 080 32.56E. CTD on deck MT
0607z 11/11/11 00 04.43N. 080 32.56E. Micro Profiler 1 deployed MT
0616z 11/11/11 00 04.43N. 080 32.56E. Micro Profiler 1 on deck MT
0621z 11/11/11 00 04.43N. 080 32.56E. Chameleon deployed astern MT
0805z 11/11/11 00 04.43N. 080 32.56E. WX balloon 24 deployed MT
0905z 11/11/11 00 04.43N. 080 32.56E. Microprofiler 2 deployed MT
0909z 11/10/11 00 04.43S. 080 32.56E. Microprofiler 2 on deck MT
1115z 11/11/11 00 04.43S. 080 29.99E. WX Balloon 25 deployed MS
1230z 11/11/11 00 04.43N. 080 32.56E. Bow CTD Chian deployed EW
1300z 11/11/11 00 04.43N. 080 32.56E. Pipe string deployed EW
1415z 11/11/11 00 04.43N. 080 32.56E. WX Balloon 26 deployed MS
1600z 11/11/11 00 04.43N. 080 32.56E. CTD 2 deployed MS
1606z 11/11/11 00 04.43N. 080 32.56E. CTD @ depth 200m MS
1615z 11/11/11 00 04.43N. 080 32.56E. CTD on deck MS
1714z 11/11/11 00 04.43N. 080 32.56E. WX Balloon 27 deployed MS
2011z 11/11/11 00 04.43N. 080 32.56E. WX Ballon 28 deployed MT
2313z 11/11/11 00 04.43N. 080 32.56E. WX Balloon #29 Deployed TD
0213z 11/12/11 00 04.94N. 080 32.04E. WX Balloon 30 deployed MS
0306z 11/12/11 00 05.27N. 080 31.75E. Microprofiler 3 deployed MS
0311z 11/12/11 00 05.31N. 080 31.73E. Microprofiler 3 on deck MS
0514z 11/12/11 00 06.08N. 080 31.11E. WX Balloon # 31 deployed MS
0606z 11/12/11 00 06.42N. 080 30.84E. Micro Profiler 4 deployed MT
0611z 11/12/11 00 06.45N. 080 30.81E. Micro Profiler 4 on deck MT
0655z 11/12/11 00 06.73N. 080 30.57E. Chameleon on deck MT
0715z 11/12/11 00 06.85N. 080 30.46E. Chameleon deployed MT
0726z 11/11/11 00 06.89N. 080 30.42E. CTD 3 deployed MT
0735z 11/12/11 00 06.89N. 080 30.43E. CTD 3 @ 302m MT
0746z 11/12/11 00 06.89N. 080 30.43E. CTD 3 on deck MT
0819z 11/12/11 00 07.10N. 080 30.25E. WX Balloon 32 deployed MT
0903z 11/12/11 00 07.31N. 080 30.07E. Microprofiler 5 deployed MT
0909z 11/11/11 00 07.31N. 080 30.07E. Microprofiler 5 on deck MT

December 7, 2011

1106z 11/12/11 00 07.31N. 080 30.07E. WX Ballon 33 deployed MT
1415z 11/12/11 00 07.31N. 080 30.07E. WX Balloon 34 deployed MS
1604z 11/12/11 00 07.31N. 080 30.08E. CTD 4 deployed MS
1625z 11/12/11 00 07.31N. 080 30.07E. CTD @ depth 305m MS
1640z 11/12/11 00 07.31N. 080 30.07E. CTD on deck MS
2027z 11/12/11 00 07.31N. 080 30.08E. WX Balloon 36 deployed MT
2316z 11/12/11 00 07.30N. 080 30.08E. WX Balloon 37 deployed TD
0215z 11/13/11 00 07.30N. 080 30.07E. WX Balloon 38 deployed MS
0301z 11/13/11 00 07.30N. 080 30.07E. Microprofiler 6 deployed MS
0306z 11/13/11 00 07.30N. 080 30.07E. Microprofiler 6 on deck MS
0509z 11/13/11 00 07.30N. 080 30.07E. WX balloon 39 deployed MS
0607z 11/13/11 00 07.30N. 080 30.07E. Microprofiler 7 deployed MT
0613z 11/13/11 00 07.30N. 080 30.07E. Microprofiler 7 on deck MT
0647z 11/13/11 00 07.30N. 080 30.07E. CTD 5 deployed MT
0651z 11/13/11 00 07.30N. 080 30.07E. Chameleon on deck MT
0701z 11/13/11 00 07.30N. 080 30.07E. CTD 5 @ 303m MT
0712z 11/13/11 00 07.30N. 080 30.08E. CTD 5 on deck MT
0715z 11/13/11 00 07.30N. 080 30.08E. Chameleon deployed MT
0812z 11/13/11 00 07.30N. 080 30.07E. WX Balloon 40 deployed MT
0848z 11/13/11 00 07.30N. 080 30.07E. Chameleon on deck MT
0906z 11/13/11 00 07.17N. 080 30.54E. Microprofiler 8 deployed MT
0912z 11/13/11 00 07.17N. 080 30.54E. Microprofiler 8 on deck MT
0913z 11/13/11 00 07.17N. 080 30.54E. Chameleon deployed MT
1109z 11/13/11 00 07.17N. 080 30.54E. WX Balloon 41 deployed MT
1409z 11/13/11 00 07.17N. 080 30.54E. WX Balloon 42 deployed MS
1600z 11/13/11 00 07.17N. 080 30.54E. CTD 6 deployed MS
1610z 11/13/11 00 07.17N. 080 30.53E. CTD @ depth 305m MS
1625z 11/13/11 00 07.17N. 080 30.54E. CTD 6 on deck MS
1752z 11/13/11 00 07.17N. 080 30.53E. WX Balloon 43 deployed MT
2020z 11/13/11 00 07.17N. 080 30.54E. WX Balloon 44 deployed MT
2322z 11/13/11 00 07.17N. 080 30.53E. WX Balloon 45 Deployed TD
0213z 11/14/11 00 07.16N. 080 30.53E. WX Balloon 46 deployed MS
0300z 11/14/11 00 07.16N. 080 30.53E. Microprofiler 9 deployed MS
0305z 11/14/11 00 07.16N. 080 30.53E. Microprofiler 9 on deck MS
0512z 11/14/11 00 07.16N. 080 30.53E. WX Balloon 47 deployed MS
0604z 11/14/11 00 07.16N. 080 30.53E. Microprofiler 10 deployed MT
0659z 11/14/11 00 07.16N. 080 30.53E. CTD 7 deployed MT
0711z 11/14/11 00 07.16N. 080 30.53E. CTD 7 @ 303m MT
0722z 11/14/11 00 07.16N. 080 30.53E. CTD 7 on deck MT
0810z 11/14/11 00 07.16N. 080 30.53E. WX Balloon 48 deployed MT
0820z 11/14/11 00 07.16N. 080 30.53E. Drifter 82314 deployed MT
0905z 11/13/11 00 07.17N. 080 30.54E. Microprofiler 11 deployed MT
0913z 11/14/11 00 07.16N. 080 30.53E. Microprofiler 11 on deck MT
1109z 11/14/11 00 07.16N. 080 30.53E. WX Ballon 49 deployed Mt
1413z 11/14/11 00 07.16N. 080 30.53E. WX Balloon 50 deployed MS
1604z 11/14/11 00 07.16N. 080 30.53E. CTD 8 deployed MS

December 7, 2011

1615z 11/14/11 00 07.16N. 080 30.53E. CTD @ depth 305m MS
1622z 11/14/11 00 07.16N. 080 30.53E. CTD 8 on deck MS
1722z 11/14/11 00 07.17N. 080 30.53E. WX Balloon 51 deployed MS
2013z 11/14/11 00 07.17N. 080 30.53E. WX Ballonn 52 deployed MT
2309Z 11/14/11 00 07.17N. 080 30.53E. WX Balloon 53 Deplyed TD
0215z 11/15/11 00 07.17N. 080 30.54E. WX Balloon 54 deployed MS
0304z 11/15/11 00 07.17N. 080 30.54E. Microprofiler 12 deployed MS
0310z 11/15/11 00 07.17N. 080 30.54E. Microprofiler 12 on deck MS
0509z 11/15/11 00 07.16N. 080 30.53E. WX Balloon 55 deployed MS
0610z 11/15/11 00 07.16N. 080 30.53E. Microprofiler 13 deployed MT
0615z 11/15/11 00 07.16N. 080 30.53E. Microprofiler 13 on deck MT
0704z 11/15/11 00 07.16N. 080 30.53E. CTD 9 deployed MT
0714z 11/15/11 00 07.16N. 080 30.53E. CTD 9 @ 304m MT
0726z 11/15/11 00 07.16N. 080 30.53E. CTD 9 on deck MT
0808z 11/15/11 00 07.17N. 080 30.54E. WX Balloon 56 deployed MT
0906z 11/15/11 00 07.17N. 080 30.53E. Microprofiler 14 deployed MT
0912z 11/15/11 00 07.16N. 080 30.53E. Microprofiler 14 on deck MT
1108z 11/15/11 00 07.17N. 080 30.54E. WX Baollon 57 deployed MT
1413z 11/15/11 00 07.17N. 080 30.54E. WX Balloon 58 deployed MS
1607z 11/15/11 00 07.17N. 080 30.54E. CTD 10 deployed MS
1617z 11/15/11 00 07.17N. 080 30.54E. CTD @ depth 304m MS
1625z 11/15/11 00 07.17N. 080 30.54E. CTD 10 on deck MS
1712z 11/15/11 00 07.17N. 080 30.53E. WX Balloon 59 deployed MS
2016z 11/15/11 00 07.17N. 080 30.53E. WX Balloon 60 deployed MT
2307z 11/15/11 00 07.17N. 080 30.54E. WX Balloon 61 deployed TD
0215z 11/16/11 00 07.17N. 080 30.54E. WX Balloon 62 deployed MS
0303z 11/16/11 00 07.17N. 080 30.54E. Microprofiler 15 deployed MS
0310z 11/16/11 00 07.17N. 080 30.54E. Microprofiler 15 on deck MS
0511z 11/16/11 00 07.17N. 080 30.54E. WX Balloon 63 deployed MS
0606z 11/16/11 00 07.16N. 080 30.53E. Microprofiler 16 deployed MT
0615z 11/16/11 00 07.16N. 080 30.53E. Microprofiler 16 on deck MT
0703z 11/16/11 00 07.17N. 080 30.53E. CTD 11 deployed MT
0714z 11/16/11 00 07.16N. 080 30.53E. CTD 11 @ 304m MT
0725z 11/16/11 00 07.17N. 080 30.54E. CTD 11 on deck MT
0808z 11/16/11 00 07.17N. 080 30.54E. WX Balloon 64 deployed MT
0903z 11/16/11 00 07.17N. 080 30.53E. Microprofiler 17 deployed MT
0912z 11/16/11 00 07.17N. 080 30.53E. Microprofiler 17 on deck MT
1108z 11/15/11 00 07.17N. 080 30.54E. WX Balloon 65 deployed MS
1413z 11/16/11 00 07.18N. 080 30.54E. WX Balloon 66 deployed MS
1607z 11/16/11 00 07.18N. 080 30.53E. CTD 12 deployed MS
1618z 11/16/11 00 07.18N. 080 30.53E. CTD @ depth 304m MS
1630z 11/16/11 00 07.18N. 080 30.54E. CTD 12 on deck MS
1715z 11/16/11 00 07.18N. 080 30.53E. WX Balloon 67 deployed MS
2015z 11/16/11 00 07.18N. 080 30.53E. WX Balloon 68 deployed MT
2312z 11/16/11 00 07.17N. 080 30.53E. WX Balloon 69 deployed TD
0215z 11/17/11 00 07.18N. 080 30.53E. WX Balloon 70 deployed MS

December 7, 2011

0304z 11/17/11 00 07.18N. 080 30.53E. Microprofiler 18 deployed MS
0310z 11/17/11 00 07.18N. 080 30.53E. Microprofiler 18 on deck MS
0510z 11/17/11 00 07.18N. 080 30.53E. WX Balloon 71 deployed MS
0610z 11/17/11 00 07.18N. 080 30.53E. Microprofiler 19 deployed MT
0615z 11/17/11 00 07.18N. 080 30.53E. Microprofiler 19 on deck MT
0708z 11/17/11 00 07.18N. 080 30.53E. CTD 13 deployed MT
0718z 11/17/11 00 07.18N. 080 30.53E. CTD 13 @ 303m MT
0730z 11/17/11 00 07.18N. 080 30.53E. CTD 13 on deck MT
0808z 11/17/11 00 07.18N. 080 30.53E. WX Balloon 72 deployed MT
0836z 11/17/11 00 07.18N. 080 30.53E. Drifter 82646 deployed MT
0905z 11/17/11 00 07.17N. 080 30.53E. Microprofiler 20 deployed MT
0909z 11/17/11 00 07.18N. 080 30.53E. Microprofiler 20 on deck MT
1103z 11/17/11 00 07.18N. 080 30.53E. WX Balloon 73 deployed MS
1410z 11/17/11 00 07.18N. 080 30.53E. WX Balloon 74 deployed MS
1607z 11/17/11 00 07.18N. 080 30.53E. CTD 14 deployed MS
1614z 11/17/11 00 07.18N. 080 30.53E. CTD @ depth 304m MS
1625z 11/17/11 00 07.18N. 080 30.53E. CTD 14 on deck MS
1713z 11/17/11 00 07.18N. 080 30.53E. WX Balloon 75 deployed MS
2016z 11/17/11 00 07.18N. 080 30.53E. WX Balloon 76 deployed MT
2315z 11/16/11 00 07.18N. 080 30.53E. WX Balloon 77 deployed TD
0023z 11/17/11 00 07.18N. 080 30.53E. CTD 15 Deployed TD
0042z 11/17/11 00 07.18N. 080 30.53E. CTD 15 aboard TD
0215z 11/18/11 00 07.18N. 080 30.53E. WX Balloon 78 deployed MS
0304z 11/18/11 00 07.18N. 080 30.53E. Microprofiler 21 deployed MS
0310z 11/18/11 00 07.18N. 080 30.53E. Microprofiler 21 on deck MS
0510z 11/18/11 00 07.18N. 080 30.53E. WX Balloon 79 deployed MS
0608z 11/18/11 00 07.18N. 080 30.53E. Microprofiler 22 deployed MT
0614z 11/18/11 00 07.18N. 080 30.53E. Microprofiler 22 on deck MT
0702z 11/18/11 00 07.18N. 080 30.53E. CTD 16 deployed MT
0703z 11/18/11 00 07.18N. 080 30.53E. Chameleon on deck MT
0713z 11/18/11 00 07.18N. 080 30.53E. CTD @ 304m MT
0724z 11/18/11 00 07.18N. 080 30.53E. CTD 16 on deck MT
0726z 11/18/11 00 07.18N. 080 30.53E. Chameleon deployed MT
0813z 11/18/11 00 07.18N. 080 30.53E. WX Balloon 80 deployed MT
0903z 11/18/11 00 07.18N. 080 30.54E. Microprofiler 23 deployed MT
0908z 11/18/11 00 07.18N. 080 30.53E. Microprofiler 23 on deck MT
1115z 11/18/11 00 07.18N. 080 30.54E. WX Balloon 81 Deployed EW
1413z 11/18/11 00 07.18N. 080 30.54E. WX Balloon 82 deployed MS
1606z 11/18/11 00 07.18N. 080 30.53E. CTD 17 deployed MS
1617z 11/18/11 00 07.18N. 080 30.53E. CTD @ depth 304m MS
1625z 11/18/11 00 07.18N. 080 30.53E. CTD 17 on deck MS
1725z 11/18/11 00 07.18N. 080 30.53E. WX Balloon 83 deployed MS
2015z 11/18/11 00 07.18N. 080 30.54E. WX Ballooon 84 deployed MT
2318z 11/18/11 00 07.17N. 080 30.54E. WX Balloon 85 deployed TD
0215z 11/19/11 00 07.17N. 080 30.54E. WX Balloon 86 deployed MS
0304z 11/19/11 00 07.18N. 080 30.53E. Microprofiler 24 deployed MS

December 7, 2011

0310z 11/19/11 00 07.18N. 080 30.53E. Microprofiler 24 on deck MS
0511z 11/19/11 00 07.17N. 080 30.54E. WX Balloon 87 deployed MS
0553z 11/19/11 00 07.17N. 080 30.54E. Chameleon deployed MT
0615z 11/19/11 00 07.17N. 080 30.54E. Miroprofiler 25 deployed MT
0620z 11/19/11 00 07.17N. 080 30.54E. Microprofiler 25 on deck MT
0703z 11/19/11 00 07.17N. 080 30.53E. CTD 18 deployed MT
0716z 11/19/11 00 07.18N. 080 30.53E. CTD 18 @ 303m MT
0727z 11/19/11 00 07.17N. 080 30.54E. CTD 18 on deck MT
0809z 11/19/11 00 07.17N. 080 30.54E. WX Balloon 88 deployed MT
0903z 11/19/11 00 07.17N. 080 30.54E. Microprofiler 26 deployed MT
0909z 11/19/11 00 07.17N. 080 30.54E. Microprofiler 26 on deck MT
1107z 11/18/11 00 07.18N. 080 30.53E. WX Balloon 89 deployed MS
1415z 11/19/11 00 07.17N. 080 30.54E. WX Balloon 90 deployed MS
1604z 11/19/11 00 07.17N. 080 30.54E. CTD 19 deployed MS
1617z 11/19/11 00 07.17N. 080 30.54E. CTD @ depth 300m MS
1625z 11/19/11 00 07.17N. 080 30.54E. CTD 19 on deck MS
1715z 11/19/11 00 07.17N. 080 30.54E. WX Balloon 91 deployed MS
2012z 11/19/11 00 07.18N. 080 30.54E. WX Balloon 92 deployed MT
2315z 11/19/11 00 07.17N. 080 30.54E. WX Balloon 93 deployed TD
0215z 11/20/11 00 07.17N. 080 30.54E. WX Balloon 94 deployed MS
0306z 11/20/11 00 07.18N. 080 30.54E. Microprofiler 26 deployed MS
0310z 11/20/11 00 07.18N. 080 30.54E. Microprofiler 26 on deck MS
0314z 11/20/11 00 07.18N. 080 30.54E. CTD 20 deployed MS
0322z 11/20/11 00 07.18N. 080 30.54E. CTD @ depth 300m MS
0331z 11/20/11 00 07.18N. 080 30.54E. CTD 20 on deck MS
0507z 11/20/11 00 07.18N. 080 30.54E. WX Balloon 95 deployed MS
0603z 11/20/11 00 07.18N. 080 30.54E. Microprofiler 27 deployed MT
0608z 11/20/11 00 07.18N. 080 30.54E. Microprofiler 27 on deck MT
0629z 11/20/11 00 07.18N. 080 30.54E. Chameleon on deck MT
0650z 11/20/11 00 07.18N. 080 30.54E. Chameleon deployed MT
0705z 11/20/11 00 07.18N. 080 30.54E. CTD 21 deployed MT
0715z 11/20/11 00 07.18N. 080 30.54E. CTD @ 303m MT
0727z 11/20/11 00 07.17N. 080 30.54E. CTD 21 on deck MT
0811z 11/20/11 00 07.17N. 080 30.54E. WX Balloon 96 deployed MT
0836z 11/20/11 00 07.17N. 080 30.54E. Drifter 44197 deployed MT
0910z 11/20/11 00 07.18N. 080 30.54E. Microprofiler 28 deployed Mt
0914z 11/20/11 00 07.17N. 080 30.54E. Microprofiler 28 on deck Mt
1110z 11/20/11 00 07.18N. 080 30.53E. WX Balloon 97 deployed <S
1410z 11/20/11 00 07.18N. 080 30.53E. WX Balloon 98 deployed MS
1607z 11/20/11 00 07.17N. 080 30.54E. CTYD 22 deployed MS
1617z 11/20/11 00 07.17N. 080 30.54E. CTD @ depth 300m MS
1625z 11/20/11 00 07.17N. 080 30.54E. CTD 22 on deck MS
1720z 11/20/11 00 07.17N. 080 30.54E. WX Balloon 99 deployed MS
2010z 11/20/11 00 07.18N. 080 30.54E. WX Balloon 100 deployed MT
2329z 11/20/11 00 07.18N. 080 30.53E. WX Balloon 101 deployed TD
0215z 11/21/11 00 07.18N. 080 30.53E. WX Balloon 102 deployed MS

December 7, 2011

0304z 11/21/11 00 07.18N. 080 30.53E. Microprofiler 29 deployed MS
0310z 11/21/11 00 07.18N. 080 30.53E. Microprofiler 29 on deck MS
0515z 11/21/11 00 07.18N. 080 30.53E. WX Balloon 103 deployed MS
0602z 11/21/11 00 07.18N. 080 30.53E. Microprofiler 20 deployed MT
0608z 11/21/11 00 07.18N. 080 30.53E. Microprofiler 30 on deck MT
0702z 11/21/11 00 07.18N. 080 30.54E. CTD 23 deployed MT
0714z 11/21/11 00 07.18N. 080 30.53E. CTD @ 300m MT
0723z 11/21/11 00 07.18N. 080 30.53E. CTD 23 on deck MT
0804z 11/21/11 00 07.18N. 080 30.53E. WX Balloon 104 deployed MT
0906z 11/21/11 00 07.18N. 080 30.53E. Microprofiler 31 deployed MT
0910z 11/21/11 00 07.18N. 080 30.53E. Microprofiler 31 on deck MT
1112z 11/21/11 00 07.18N. 080 30.53E. WX Balloon 105 deployed MT
1410z 11/21/11 00 07.18N. 080 30.53E. WX Balloon 106 deployed MS
1604z 11/21/11 00 07.17N. 080 30.54E. CTD 24 deployed MS
1615z 11/21/11 00 07.17N. 080 30.54E. CTD @ depth 300m MS
1625z 11/21/11 00 07.18N. 080 30.54E. CTD 24 on deck MS
1713z 11/21/11 00 07.17N. 080 30.54E. WX Balloon 107 deployed MS
1826z 11/21/11 00 07.17N. 080 30.54E. Chameleon on deck MT
1925z 11/21/11 00 07.17N. 080 30.54E. Chameleon deployed MT
0203z 11/21/11 00 07.18N. 080 30.53E. CTD 25 deployed MT
0212z 11/21/11 00 07.18N. 080 30.53E. WX Balloon 108 deployed MT
2016z 11/21/11 00 07.18N. 080 30.53E. CTD @ 300m MT
2028z 11/21/11 00 07.18N. 080 30.54E. CTD 25 on deck MT
2308z 11/21/11 00 07.17N. 080 30.53E. WX Balloon 109 deployed TD
2314z 11/21/11 00 07.17N. 080 30.53E. CTD 26 Deployed TD
2332z 11/21/11 00 07.17N. 080 30.53E. CTD 26 Recovered TD
0215z 11/22/11 00 07.15N. 080 30.52E. WX Balloon 110 deployed MS
0304z 11/22/11 00 07.15N. 080 30.52E. Microprofiler 31 deployed MS
0310z 11/22/11 00 07.16N. 080 30.52E. Microprofiler 31 on deck MS
0510z 11/22/11 00 07.15N. 080 30.52E. WX Balloon 111 deployed MS
0601z 11/22/11 00 07.15N. 080 30.52E. Microprofiler 32 deployed MT
0606z 11/22/11 00 07.15N. 080 30.52E. Microprofiler 32 on deck MT
0703z 11/22/11 00 07.15N. 080 30.52E. CTD 27 deployed MT
0712z 11/21/11 00 07.18N. 080 30.53E. CTD 27 @ 300m MT
0720z 11/22/11 00 07.15N. 080 30.52E. CTD 27 on deck MT
0812z 11/22/11 00 07.15N. 080 30.52E. WX Balloon 112 deployed MT
0908z 11/22/11 00 07.18N. 080 30.53E. Microprofiler 33 deployed MT
0912z 11/22/11 00 07.18N. 080 30.53E. Microprofiler 33 on deck MT
1111z 11/22/11 00 07.18N. 080 30.53E. WX Balloon 113 deployed MT
1410z 11/22/11 00 07.15N. 080 30.52E. WX Balloon 114 deployed MS
1603z 11/22/11 00 07.15N. 080 30.52E. CTD 28 deployed MS
1616z 11/22/11 00 07.15N. 080 30.52E. CTD @ depth 300m MS
1625z 11/22/11 00 07.15N. 080 30.52E. CTD 28 on deck MS
1728z 11/22/11 00 07.15N. 080 30.52E. WX Balloon 115 deployed MS
2011z 11/22/11 00 07.15N. 080 30.52E. WX Balloon 116 deployed MT
2307z 11/22/11 00 07.17N. 080 30.54E. WX Balloon 117 deployed TD

December 7, 2011

0215z 11/23/11 00 07.15N. 080 30.52E. WX Balloon 119 deployed MS
0302z 11/23/11 00 07.15N. 080 30.52E. Microprofiler 34 deployed MS
0308z 11/23/11 00 07.15N. 080 30.52E. Microprofiler 34 on deck MS
0510z 11/23/11 00 07.15N. 080 30.52E. WX Balloon 120 deployed MS
0606z 11/23/11 00 07.15N. 080 30.53E. Microprofiler 35 deployed MT
0610z 11/23/11 00 07.15N. 080 30.53E. Microprofiler 35 on deck MT
0704z 11/23/11 00 07.15N. 080 30.52E. CTD 29 deployed MT
0712z 11/23/11 00 07.15N. 080 30.52E. CTD @ 300m MT
0720z 11/23/11 00 07.15N. 080 30.52E. CTD on deck MT
0814z 11/22/11 00 07.15N. 080 30.52E. WX Balloon 121 deployed MT
0830z 11/23/11 00 07.15N. 080 30.52E. Drifter 44216 deployed MT
0905z 11/23/11 00 07.15N. 080 30.52E. Microprofiler 36 deployed MT
0910z 11/23/11 00 07.15N. 080 30.52E. Microprofiler 36 on deck MT
1110z 11/23/11 00 07.15N. 080 30.52E. WX Balloon 122 deployed MT
1415z 11/23/11 00 07.15N. 080 30.53E. WX Balloon 123 deployed MS
1602z 11/23/11 00 07.15N. 080 30.52E. CTD 30 deployed MS
1614z 11/23/11 00 07.15N. 080 30.52E. CTD @ depth 300m MS
1623z 11/23/11 00 07.15N. 080 30.52E. CTD 30 on deck MS
1729z 11/23/11 00 07.15N. 080 30.52E. WX Balloon 124 deployed MS
2013z 11/23/11 00 07.15N. 080 30.53E. WX Balloon 125 deployed MT
2309z 11/23/11 00 07.15N. 080 30.52E. WX Balloon 126 deployed TD
0215z 11/24/11 00 07.15N. 080 30.52E. WX Balloon 127 deployed MS
0305z 11/24/11 00 07.16N. 080 30.53E. Microprofiler 37 deployed MS
0310z 11/24/11 00 07.16N. 080 30.53E. Microprofiler 37 on deck MS
0515z 11/24/11 00 07.16N. 080 30.53E. Wx Balloon 128 deployed MS
0558z 11/24/11 00 07.16N. 080 30.53E. Microprofiler 38 deployed MT
0603z 11/24/11 00 07.16N. 080 30.53E. Microprofiler 38 on deck MT
0706z 11/24/11 00 07.16N. 080 30.53E. CTD 31 deployed MT
0716z 11/24/11 00 07.16N. 080 30.53E. CTD @ 300m MT
0728z 11/24/11 00 07.16N. 080 30.53E. CTD 31 on deck MT
0810z 11/24/11 00 07.16N. 080 30.53E. WX Balloon 129 deployed MT
0906z 11/24/11 00 07.16N. 080 30.53E. Microprofiler 39 deployed MT
0910z 11/24/11 00 07.16N. 080 30.53E. Mciroprofiler 39 on deck MT
1110z 11/24/11 00 07.15N. 080 30.52E. WX Balloon 130 deployed MT
2012z 11/23/11 00 07.15N. 080 30.52E. WX Balloon 131 deployed MT
2308z 11/24/11 00 07.22N. 080 29.77E. WX Balloon 134 deployed TD
2321z 11/24/11 00 07.22N. 080 29.77E. WX Balloon 135 deployed TD
0215z 11/25/11 00 07.23N. 080 29.77E. WX Balloon 135 deployed MS
0246z 11/25/11 00 07.23N. 080 29.77E. T-chain on deck MS\
0304z 11/25/11 00 07.22N. 080 29.77E. CTD 32 deployed MS
0914z 11/25/11 00 07.16N. 080 30.53E. CTd @ depth 300m MS
0325z 11/25/11 00 07.22N. 080 29.77E. CTD 32 on deck MS
0335z 11/25/11 00 07.21N. 080 29.74E. Chameleon on deck MS
0441z 11/25/11 00 07.48N. 080 35.15E. Chameleon deployed MS
0529z 11/25/11 00 07.46N. 080 35.17E. WX Balloon 136 deployed MS
0603z 11/25/11 00 07.47N. 080 35.17E. Microprofiler 40 deployed MT

December 7, 2011

0610z 11/25/11 00 07.47N. 080 35.17E. Microprofiler 40 on deck MT
0705z 11/25/11 00 07.47N. 080 35.17E. CTD 33 deployed MT
0715z 11/25/11 00 07.47N. 080 35.17E. CTD @ 300m MT
0729z 11/25/11 00 07.47N. 080 35.17E. CTD 33 on deck MT
0810z 11/25/11 00 07.47N. 080 35.17E. WX Balloon 137 deployed MT
0905z 11/25/11 00 07.47N. 080 35.17E. Microprofiler 41 deployed MT
0911z 11/25/11 00 07.47N. 080 35.17E. Microprofiler 41 on deck MT
1110z 11/25/11 00 07.47N. 080 35.17E. WX Balloon 138 deployed MT
1230z 11/25/11 00 07.47N. 080 35.17E. Chain CTD Deployed EW
1415z 11/25/11 00 07.47N. 080 35.17E. WX Balloon 139 deployed MS
1602z 11/25/11 00 07.47N. 080 35.17E. CTD 33 deployed <S
1614z 11/25/11 00 07.47N. 080 35.17E. CTD @ depth 300m MS
1625z 11/25/11 00 07.47N. 080 35.17E. CTD 33 on deck MS
1715z 11/25/11 00 07.47N. 080 35.17E. WX Balloon 140 deployed MS
2013z 11/25/11 00 07.47N. 080 35.17E. WX Balloon 141 deployed MT
2321z 11/25/11 00 07.47N. 080 35.17E. WX Balloon 142 Deployed TD
0212z 11/26/11 00 07.47N. 080 35.17E. WX Balloon 143 deployed MS
0306z 11/26/11 00 07.47N. 080 35.17E. Microprofiler 41 deployed MS
0312z 11/26/11 00 07.47N. 080 35.17E. Microprofiler 41 on deck MS
0512z 11/26/11 00 07.47N. 080 35.17E. WX Balloon 144 deployed MS
0605z 11/26/11 00 07.47N. 080 35.17E. Microprofiler 42 deployed MT
0611z 11/26/11 00 07.47N. 080 35.17E. Microprofiler 42 on deck MT
0702z 11/26/11 00 07.47N. 080 35.17E. CTD 35 deployed MT
0711z 11/26/11 00 07.47N. 080 35.17E. CTD @ 300m MT
0723z 11/26/11 00 07.47N. 080 35.17E. CTD 35 on deck MT
0810z 11/26/11 00 07.47N. 080 35.17E. WX Balloon 145 deployed MT
0839z 11/26/11 00 07.47N. 080 35.17E. Drifter 44214 deployed MT
0841z 11/26/11 00 07.47N. 080 35.17E. WX Balloon 146 deployed MT
0906z 11/26/11 00 07.47N. 080 35.17E. Microprofiler 43 deployed MT
0912z 11/26/11 00 07.47N. 080 35.17E. Microprofiler 43 on deck MT
1101z 11/26/11 00 07.47N. 080 35.17E. Wx Balloon 147 deployed MS
1405z 11/26/11 00 07.47N. 080 35.17E. WX Balloon 148 deployed MS
1610z 11/26/11 00 07.47N. 080 35.17E. CTD 36 deployed MS
1622z 11/26/11 00 07.47N. 080 35.17E. CTD @ depth 300m MS
1630z 11/26/11 00 07.47N. 080 35.17E. CTD 36 on deck MS
2018z 11/26/11 00 07.47N. 080 35.17E. WX Balloon 150 deployed MT
2311z 11/26/11 00 07.47N. 080 35.17E. WX Balloon 150 Deployed TD
0205z 11/27/11 00 07.47N. 080 35.17E. Wx Balloon 152 deployed MS
0302z 11/27/11 00 07.47N. 080 35.17E. Microprofiler 44 deployed MS
0310z 11/27/11 00 07.47N. 080 35.17E. Microprofiler 44 on deck MS
0505z 11/27/11 00 07.47N. 080 35.17E. Wx Balloon 153 deployed MS
0601z 11/27/11 00 07.47N. 080 35.17E. Microprofiler 45 deployed MT
0606z 11/27/11 00 07.47N. 080 35.17E. Microprofiler 45 on deck MT
0703z 11/27/11 00 07.47N. 080 35.17E. CTD 37 deployed MT
0714z 11/27/11 00 07.47N. 080 35.17E. CTD @ 300m MT
0725z 11/27/11 00 07.47N. 080 35.17E. CTD 37 on deck MT

December 7, 2011

0810z 11/27/11 00 07.47N. 080 35.17E. WX Balloon 154 deployed MT
0905z 11/27/11 00 07.47N. 080 35.17E. Microprofiler 46 deployed MT
0913z 11/27/11 00 07.47N. 080 35.17E. Microprofiler 46 on deck MT
1108z 11/27/11 00 07.47N. 080 35.17E. WX Balloon 155 deployed MS
2012z 11/27/11 00 07.47N. 080 35.17E. WX Ballon 157 deployed MT
2313z 11/27/11 00 07.47N. 080 35.17E. WX Balloon 158 deployed TD
0208z 11/28/11 00 07.47N. 080 35.17E. WX Balloon 159 deployed MS
0301z 11/28/11 00 07.47N. 080 35.17E. Microprofiler 47 deployed Ms
0308z 11/28/11 00 07.47N. 080 35.17E. Microprofiler 47 on deck MS
0515z 11/28/11 00 07.46N. 080 35.17E. WX Balloon 160 deployed MS
0605z 11/28/11 00 07.46N. 080 35.17E. Microrprofiler 48 deployed MT
0706z 11/28/11 00 07.46N. 080 35.17E. CTD 39 deployed MT
0716z 11/28/11 00 07.46N. 080 35.17E. CTD @ 300m MT
0729z 11/28/11 00 07.46N. 080 35.17E. CTD 39 on deck MT
0807z 11/28/11 00 07.46N. 080 35.17E. WX Balloon 161 deployed MT
0909z 11/28/11 00 07.46N. 080 35.17E. Microprofiler 49 deployed MT
0916z 11/28/11 00 07.46N. 080 35.17E. Microprofiler 49 on deck MT
1108z 11/28/11 00 07.46N. 080 35.17E. WX Balloon 162 deployed <S
1415z 11/28/11 00 07.46N. 080 35.17E. WX Balloon 163 deployed MS
1551z 11/28/11 00 07.46N. 080 35.17E. Chameleon on deck MS
1602z 11/28/11 00 07.46N. 080 35.17E. CTD 40 deployed MS
1614z 11/28/11 00 07.47N. 080 35.17E. CTD @ depth 300m MS
1623z 11/28/11 00 07.46N. 080 35.17E. CTD 40 on deck MS
1645z 11/28/11 00 07.46N. 080 35.17E. Chameleon deployed MS
1715z 11/28/11 00 07.46N. 080 35.17E. WX Balloon 164 deployed MS
2008z 11/28/11 00 07.46N. 080 35.17E. WX Balloon 165 deployed MT
2312z 11/28/11 00 07.46N. 080 35.17E. WX Balloon 166 deployed TD
0100z 11/29/11 00 07.46N. 080 35.17E. CTD 41 Deployed TD
0118z 11/29/11 00 07.46N. 080 35.17E. CTD 41 aboard TD
0608z 11/29/11 00 07.46N. 080 35.17E. Microprofiler 51 deployed MT
0614z 11/29/11 00 07.46N. 080 35.17E. Microprofiler 51 on deck MT
0703z 11/29/11 00 07.46N. 080 35.17E. CTD 42 deployed MT
0713z 11/29/11 00 07.46N. 080 35.17E. CTD @ 300m MT
0728z 11/29/11 00 07.46N. 080 35.17E. CTD 42 on deck MT
0808z 11/29/11 00 07.46N. 080 35.17E. Wx Balloon 169 deployed MT
0831z 11/29/11 00 07.46N. 080 35.17E. Drifter 44195 deployed MT
0914z 11/29/11 00 07.46N. 080 35.17E. Microprofiler 52 deployed MT
0920z 11/29/11 00 07.46N. 080 35.17E. Microprofiler 52 on deck Mt
1415z 11/29/11 00 07.46N. 080 35.17E. WX Balloon 171 deployed MS
1602z 11/29/11 00 07.46N. 080 35.17E. CTD 43 deployed MS
1615z 11/29/11 00 07.46N. 080 35.17E. CTD @ depth 300m MS
1626z 11/29/11 00 07.46N. 080 35.17E. CTD 43 on deck MS
1715z 11/29/11 00 07.46N. 080 35.17E. WX Balloon 172 deployed MS
2015z 11/29/11 00 07.46N. 080 35.17E. WX Balloon 173 deployed MT
2318z 11/29/11 00 07.46N. 080 35.17E. WX Balloon 174 deployed TD
0302z 11/30/11 00 07.46N. 080 35.17E. Microprofiler 53 deployed MS

December 7, 2011

0602z 11/30/11 00 07.46N. 080 35.17E. Microprofiler 54 deployed MT
0609z 11/30/11 00 07.46N. 080 35.17E. Microprofiler 54 on deck MT
0706z 11/30/11 00 07.46N. 080 35.17E. CTD 44 deployed MT
0716z 11/30/11 00 07.46N. 080 35.17E. CTD 44 @ 300m MT
0725z 11/30/11 00 07.46N. 080 35.17E. CTD 44 on deck MT
0908z 11/30/11 00 07.46N. 080 35.17E. Microprofiler 55 deployed MT
1113z 11/30/11 00 07.46N. 080 35.17E. WX Balloon 176 deployed MS
1606z 11/30/11 00 07.46N. 080 35.17E. CTD 45 deployed MS
1615z 11/30/11 00 07.46N. 080 35.17E. CTD 45 @ depth 220m MS
1623z 11/30/11 00 07.46N. 080 35.17E. CTD 45 on deck MS
1708z 11/30/11 00 07.46N. 080 35.17E. WX Balloon 177 deployed MS
2018z 11/30/11 00 07.46N. 080 35.17E. WX Balloon 178 deployed MT
2310z 11/30/11 00 07.46N. 080 35.17E. WX Balloon 179 deployed TD
0601z 12/01/11 00 07.22N. 080 36.43E. Microprofiler 57 deployed MT
0606z 12/01/11 00 07.22N. 080 36.43E. Microprofiler 57 on deck MT
0705z 12/01/11 00 07.22N. 080 36.43E. CTD 46 deplyed MT
0714z 12/01/11 00 07.22N. 080 36.43E. CTD @ 220m MT
0724z 12/01/11 00 07.22N. 080 36.43E. CTD 46 on deck Mt
0908z 12/01/11 00 07.22N. 080 36.43E. Microprofiler 58 deployed MT
0915z 12/01/11 00 07.22N. 080 36.43E. Microprofiler 58 on deck Mt
1112z 12/01/11 00 07.22N. 080 36.43E. WX Balloon 181 deployed MT
1606z 12/01/11 00 07.22N. 080 36.43E. CTD 47 deployed MS
1615z 12/01/11 00 07.22N. 080 36.43E. CTD @ depth 220m MS
1625z 12/01/11 00 07.22N. 080 36.43E. CTD 47 on deck MS
1715z 12/01/11 00 07.22N. 080 36.43E. WX Balloon 182 deployed MS
2319z 12/01/11 00 07.23N. 080 36.43E. WX Balloon 183 Deployed TD
0302z 12/02/11 00 07.23N. 080 36.43E. Microprofiler 59 deployed MS
0310z 12/02/11 00 07.23N. 080 36.43E. Microprofiler 59 on deck MS
0515z 12/02/11 00 07.23N. 080 36.43E. WX Balloon 184 deployed Ms
0603z 12/02/11 00 07.23N. 080 36.43E. Microprofiler 60 deployed MT
0615z 12/02/11 00 07.23N. 080 36.43E. Microprofiler 60 on deck Mt
0702z 12/02/11 00 07.23N. 080 36.43E. CTD 48 deployed MT
1312z 12/02/11 00 07.22N. 080 36.43E. CTD @ 220m MT
0721z 12/02/11 00 07.22N. 080 36.43E. CTD 48 on deck MT
0828z 12/02/11 00 07.23N. 080 36.43E. Drifter 82651 deployed MT
0900z 12/02/11 00 07.22N. 080 36.43E. Microprofiler 61 deployed MT
1509z 12/01/11 00 07.22N. 080 36.43E. Microprofiler 61 on deck MT
0917z 12/02/11 00 07.23N. 080 36.43E. Chameleon on deck Mt
0937z 12/02/11 00 07.22N. 080 36.43E. Chain CTD on deck MT
1103z 12/02/11 00 07.23N. 080 36.40E. WX Balloon 185 deployed MT
1206z 12/02/11 00 07.22N. 080 36.40E. CTD 49 deployed EW
1230Z 12/02/11 00 07.22N. 080 36.40E. CTD 49 at 1200m EW
1259z 12/02/11 00 07.22N. 080 36.40E. CTD 49 on deck EW
1310z 12/02/11 00 07.23N. 080 36.28E. Pipe String on deck EW
1756z 12/02/11 00 59.97N. 080 30.00E. CTD 50 (D2) deployed MT
1822z 12/02/11 00 59.96N. 080 30.00E. CTD @ 1200m MT

December 7, 2011

1850z 12/02/11 00 59.97N. 080 30.00E. CTD 50 (D2) on deck MT
2315z 12/02/11 01 54.26N. 080 29.99E. WX Balloon 186 deployed TD
2353z 12/02/11 02 00.03N. 080 30.01E. CTD D3 deployed TD
0510z 12/03/11 01 03.14N. 080 30.00E. WX Balloon 187 deployed MS
1110z 12/03/11 00 12.01S. 080 30.01E. Wx Balloon 188 deployed MT
1522z 12/03/11 00 59.87S. 080 30.01E. CTD 52 deployed MS
1530z 12/03/11 00 59.86S. 080 30.01E. Drifter 82312 deployed MS
1553z 12/03/11 00 59.87S. 080 30.01E. CTD @ depth 1200m MS
1623z 12/03/11 00 59.90S. 080 30.01E. CTD 52 on deck MS
1707z 12/03/11 01 08.66S. 080 30.00E. WX Balloon 188 deployed MS
2125z 12/03/11 01 59.97S. 080 30.03E. D5 CTD deployed MT
2131z 12/03/11 01 59.97S. 080 30.03E. Drifter 44144 deployed MT
2132z 12/03/11 01 59.97S. 080 30.03E. Drifter 44147 deployed MT
2156z 12/02/11 01 37.76N. 080 29.99E. CTD D5 at depth 1200m TD
2222z 12/03/11 01 59.97S. 080 30.01E. CTD D5 on deck TD
2315z 12/03/11 01 49.21S. 080 30.00E. WX Balloon 190 deployed TD
0515z 12/04/11 00 32.12S. 080 30.00E. WX Balloon 191 deployed MS
1106z 12/04/11 00 00.01N. 081 18.79E. WX Balloon 192 deployed MT
1415z 12/04/11 00 00.02N. 082 00.09E. CTD D6 deployed MS
1443z 12/04/11 00 00.02N. 082 00.06E. CTD @ depth 1200m MS
1510z 12/04/11 00 00.01S. 082 00.12E. CTD D6 on deck MS
1715z 12/04/11 00 00.00N. 082 28.66E. WX Balloon 193 deployed MS
2316z 12/03/11 01 48.99S. 080 30.00E. WX Balloon 194 deployed TD
0017z 12/04/11 01 35.94S. 080 30.01E. CTD D7 deployed TD
0040z 12/05/11 00 00.08S. 084 00.02E. CTD D7 max depth 1200m TD
0101z 12/05/11 00 00.09S. 084 00.02E. CTD D7 on deck TD
0510z 12/05/11 00 00.00S. 084 51.59E. WX Balloon 195 deployed MS
1032z 12/05/11 00 00.09S. 086 00.13E. CTD D8 deployed EW
1058z 12/05/11 00 00.09S. 086 00.13E. D8 @ 1200m MT
1106z 12/05/11 00 00.09S. 086 00.13E. Wx Balloon 196 deployed MT
1124z 12/05/11 00 00.09S. 086 00.13E. D8 on deck MT
2035z 12/05/11 00 00.01S. 088 00.03E. D9 deployed MT
2103z 12/05/11 00 00.01S. 088 00.03E. D9 @ 1200m MT
0331z 12/05/11 00 00.01N. 088 00.03E. D9 on deck MT
2320z 12/04/11 00 00.00S. 083 49.67E. WX Balloon #198 deployed TD
0506z 12/06/11 00 00.00S. 089 34.13E. WX Balloon #199 deployed MS
0718z 12/06/11 00 00.00S. 090 00.02E. D10 deployed MT
0744z 12/06/11 00 00.00S. 090 00.02E. D10 @ 1200m MT
0810z 12/06/11 00 00.00S. 090 00.01E. D10 on deck MT
1110z 12/06/11 00 37.49S. 089 59.99E. WX Balloon #200 deployed MS
1300z 12/06/11 01 00.03S. 090 00.00E. CTD D11 deployed EW
1330z 12/06/11 01 00.03S. 090 00.00E. CTD D11 at 1200m EW
1356z 12/06/11 01 00.01S. 089 59.98E. CTD D11 on deck MS
1715z 12/06/11 01 41.18S. 090 00.00E. WX balloon #201 deployed MS
1857z 12/06/11 02 00.01S. 090 00.08E. D12 deployed MT
1921z 12/06/11 02 00.01S. 090 00.08E. D12 @ 1200m MT

December 7, 2011

1948z 12/06/11 02 00.01S. 090 00.07E. D12 on deck MT
2334z 12/05/11 00 00.01N. 088 24.78E. WX Balloon #202 deployed TD
0508z 12/07/11 00 07.76S. 090 00.00E. WX Balloon #203 deployed MS
1055z 12/07/11 01 00.03N. 090 00.05E. CTD D13 deployed EW
1110z 12/07/11 01 00.03N. 090 00.05E. WX Balloon #204 deployed EW
1119z 12/07/11 01 00.03N. 090 00.05E. CTD D13 at 1200m EW
1146z 12/07/11 01 00.06N. 090 00.04E. CTD D13 on deck EW
2323z 12/06/11 01 17.13S. 089 59.99E. WX Balloon #204 deployed TD